*Downloaded from UvA-DARE, the institutional repository of the University of Amsterdam (UvA)*
*http://hdl.handle.net/11245/2.2213*

File ID uvapub:2213
Filename 23185y.pdf
Version unknown

SOURCE (OR PART OF THE FOLLOWING SOURCE):
Type article
Title Theory of semi-ballistic wave propagation
Author(s) A.P. Mosk, T.M. Nieuwenhuizen, C.L. Barnes
Faculty FNWI: Van der Waals-Zeeman Institute (WZI)
Year 1996

FULL BIBLIOGRAPHIC DETAILS:
http://hdl.handle.net/11245/1.130244

*Copyright*

*It is not permitted to download or to forward/distribute the text or part of it without the consent of the author(s) and/or copyright holder(s), other than for strictly personal, individual use, unless the work is under an open content licence (like Creative Commons).*

*UvA-DARE is a service provided by the library of the University of Amsterdam (http://dare.uva.nl)*
*(pagedate: 2014-11-14)*

# Theory of semiballistic wave propagation

A. Mosk and Th. M. Nieuwenhuizen
*Van der Waals–Zeeman Instituut, Valckenierstraat 65-67, 1018 XE Amsterdam, The Netherlands*

C. Barnes
*Cavendish Laboratory, University of Cambridge, Madingley Road, Cambridge CB3 OHE, United Kingdom*
(Received 11 January 1996)

Wave propagation through waveguides, quantum wires, or films with a modest amount of disorder is in the semiballistic regime when in the transversal direction(s) almost no scattering occurs, while in the long direction(s) there is so much scattering that the transport is diffusive. For such systems, randomness is modeled by an inhomogeneous density of pointlike scatterers. These are first considered in the second order Born approximation and then beyond that approximation. In the latter case, it is found that attractive point scatterers in a cavity always have geometric resonances, even for Schrödinger wave scattering. In the long sample limit, the transport equation is solved analytically. Various geometries are considered: waveguides, films, and tunneling geometries such as Fabry-Pérot interferometers and double-barrier quantum wells. The predictions are compared with new and existing numerical data and with experiment. The agreement is quite satisfactory. [S0163-1829(96)00923-X]

## I. INTRODUCTION

As is empirically known from the ancient development of music instruments, cavity resonances determine the transmission of waves through devices that have dimensions of the order of the wavelength. The resonances give rise to transmission peaks of diverse systems such as flutes, organ pipes, Fabry-Pérot interferometers, electronic nanostructures,[1] and electronic waveguides. In these systems, the transmission of waves can drastically increase if the wave vector of the incoming waves allows for a new mode to be resonant. In the case of a very pure or very small cavity, impurity scattering can be neglected and the transmission is said to be ballistic. Ballistic transport has been shown to occur in various systems, including quantum point contacts[2] and narrow optical slits.[3]

For wave propagation through waveguides or quantum wires with a modest amount of disorder, several regimes occur. For rather clean systems, one still has ballistic transport of essentially unscattered waves. In the limit of dirty, but nonabsorptive and phase coherent systems, the intensity mainly diffuses through the system. As pointed out recently by one of us, for long wires or thin films there is a third regime, the semiballistic regime.[4] Here, disorder is large enough to cause diffusion in the long direction(s), but small enough to maintain ballistic motion in the narrow directions. In the present work, we shall focus on this regime.

For electronic systems the conductance can be expressed by the Landauer formula,

$$G=\frac{2e^2}{h}\sum_{\mathbf{ab}} \mathcal{T}_{\mathbf{ab}}^{\mathrm{flux}},$$

in terms of the flux transmission coefficients $\mathcal{T}_{\mathbf{ab}}^{\mathrm{flux}}$ of the system, where **a** and **b** stand for the incoming and outgoing channels, respectively. In the ballistic regime, there is no channel-to-channel scattering and the transmission coefficients are diagonal in mode space. They are of order unity for the propagating modes (the low-order cavity resonances that can be excited at the energy of the incoming wave), and exponentially small for the evanescent modes (the higher-order cavity resonances). Whenever a new cavity mode becomes resonant, the conductance makes a step of universal height $2e^2/h$.

It is well known that multiple scattering by a large density of impurities changes this ballistic transport to a diffusive one. In the diffusive regime, all intensity is completely randomly distributed over the system.

In the intermediate regime of *semiballistic transport*, a moderate amount of scatterers is present. On one hand, the cavity modes of the pure system are hardly perturbed while, on the other hand, multiple scattering dominates transport in the long direction(s).

In such systems, interesting effects appear especially near the onset of new resonances. The conductance of a quantum wire shows a dip just before a new mode becomes resonant.[5–7] Certain GaAs/$Al_xGa_{1-x}As$ double-barrier quantum wells show diffusive broadening of their transmission resonance.[8]

We study the average transmission properties of semiballistic systems using the scalar wave approximation in the limit of point scatterers. We assume that neither finite-temperature effects nor Anderson localization are relevant.

In Ref. 4, one of the authors discussed a model to explain the transport properties of these systems. In the present work, we will present the derivations of the results in that paper and extend the approach beyond the second order Born approximation to the $t$ matrix.

The setup of this paper is as follows: In Sec. II, we will calculate the transmission coefficients of a long, moderately disordered waveguide, to supply the derivation of the results presented in Ref. 4. We then apply them to the calculation of the conductivity of disordered quantum wires.

 © 1996 The American Physical Society

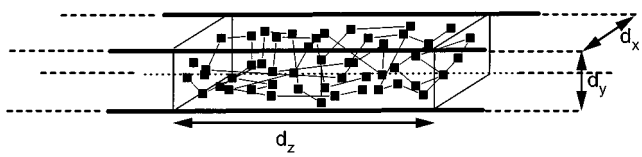


FIG. 1. The waveguide (with cross secion $d_x d_y$) is infinitely long, but the disorder is only present in a finite section of length $d_z$. The infinitely long pure sections act as ideal quantum leads.

In Sec. IV, the transmission of semiballistic double-barrier structures is examined. Ballistic double-barrier structures have a transmission peaked at certain discrete wave vectors. In the semiballistic regime, there is a broadening of these transmission resonances, and transmission to all other resonant channels. In Sec. V, we extend the discussion to include resonance effects of the scatterers that may be induced by the geometry. In Sec. VI, we discuss the comparison between our model and numerical simulations of an Anderson model in the semiballistic regime. We close with a summary.

## II. SEMIBALLISTIC TRANSPORT IN A WAVEGUIDE

We first consider the case of a moderately disordered rectangular waveguide. To simplify the problem, we consider scalar waves instead of vector waves, thus neglecting polarization effects. In this way, we model the propagation of TE modes in electromagnetic waveguides. The same approach also applies to electron propagation in quantum wires and, to some extent, sound propagation in long corridors.

Our geometry has also been chosen as simple as possible. It consists of an infinitely long waveguide within the middle a section of finite length in which a moderate amount of scatterers is present (see Fig. 1). Outside the disordered region, we have a clean system (perfect leads, for electronic systems) in which ballistic transport occurs. In the disordered region semiballistic transport occurs. Here, we consider (longitudinal) transport inside such a geometry, so that the wall potentials can be considered infinitely high. In later sections, we consider (tranverse) tunneling through such a device and its boundaries. For that application, the wall potentials must have a finite strength.

### A. The pure system

Our waveguide consists of four conducting plates, at $x=0$, $x=d_x$, $y=0$, and $y=d_x$, and it is infinite in the $z$ direction. The conducting plates impose the boundary condition $\Psi=0$ at their surface, to describe TE waves:

$$\psi(0,y,z)=\psi(d_x,y,z)=0,$$

$$\psi(x,0,z)=\psi(x,d_y,z)=0. \tag{2.1}$$

For electron propagation, this would correspond to infinite wall potentials. We assume that monochromatic waves of frequency $\omega_0$, and free space wave vector $k_0$ propagate through the guide. In the scalar wave approximation, this is described by the following equation:

$$\{-\nabla^2-k_0^2\}\psi(\mathbf{r})=0. \tag{2.2}$$

In the absence of impurities, the waves traveling through the guide have the form

$$\psi(x,y,z)=\sum_{\mathbf{p}} \Psi_{\mathbf{p}}(\boldsymbol{\rho})e^{iq_{\mathbf{p}}z}, \tag{2.3}$$

where $\boldsymbol{\rho}=(x,y)$ is the transversal position and $\Psi_{\mathbf{p}}(\boldsymbol{\rho})$ are the discrete transversal eigenmodes of the system:

$$\Psi_{\mathbf{p}}(\boldsymbol{\rho})=\sqrt{\frac{2}{d_x}}\sin(p_x x)\sqrt{\frac{2}{d_y}}\sin(p_y y), \tag{2.4}$$

$$p_x=\frac{m_x\pi}{d_x}\quad p_y=\frac{m_y\pi}{d_y}\qquad (m_{x,y}\geqslant 1;\ m_{x,y}\ \text{is an integer}).$$

Other geometries, e.g., cylindrical waveguides, can be described in the same way by substituting the corresponding mode wave functions for $\Psi$. The modes for which $\mathbf{p}^2<k_0^2$, are ''free,'' i.e., they can propagate in the $z$ direction, with the mode-dependent wave number $q_{\mathbf{p}}=\sqrt{k_0^2-\mathbf{p}^2}$. The Green's function of this pure system, to be denoted as $G^0$, is the solution of the equation

$$\{-\nabla^2-k_0^2\}G^0(\mathbf{r},\mathbf{r}')=\delta(\mathbf{r}-\mathbf{r}'), \tag{2.5}$$

with the boundary conditions (2.1). To incorporate the boundary conditions in the equation, we study the projections $G^0_{\mathbf{p}}$,

$$G^0_{\mathbf{p}}(z,z')=\int d\boldsymbol{\rho}d\boldsymbol{\rho}'\Psi^*_{\mathbf{p}}(\boldsymbol{\rho})G^0(\boldsymbol{\rho};z,\boldsymbol{\rho}';z')\Psi_{\mathbf{p}}(\boldsymbol{\rho}'). \tag{2.6}$$

Since we have translational invariance, we can use a Fourier transform to find from (2.5):

$$G^0_{\mathbf{p}}(q)=\frac{1}{q^2+\mathbf{p}^2-k_0^2-i0}. \tag{2.7}$$

The extra term $i0$ ensures convergence of the back transformation. In real space one has

$$G^0_{\mathbf{p}}(z-z')=\frac{i\exp\{i\sqrt{k_0^2-\mathbf{p}^2}|z-z'|\}}{2\sqrt{k_0^2-\mathbf{p}^2}}. \tag{2.8}$$

### B. Adding impurities

Now suppose a small density of scattering impurities is present at random positions $\mathbf{R}_i$ in the region $0\leqslant z\leqslant d_z$. Their scattering properties can be expressed in a scattering potential $V(\mathbf{r})=\Sigma_i V_s(\mathbf{r}-\mathbf{R}_i)$. We replace the single scatterer potential $V_s$ by a $\delta$ potential with scattering strength $-u$. This is known to be a good approximation for electron scattering off a screened charge. The density of scatterers

$$n(\mathbf{r})=\begin{cases} n(x,y), & 0<z<d_z \\ 0, & z<0,\ z>d_z \end{cases} \tag{2.9}$$

needs not be homogeneous in the $x,y$ directions, we will assume though that it is independent of $z$ for $0\leqslant z\leqslant d_z$. The density of scatterers will be assumed to be so small that the cavity modes (2.4) are still well defined, i.e., the scattering

mean free path $l_{\mathbf{p}}$ must be much larger than the transversal sizes $d_x, d_y$. The wave equation for this system is

$$\left\{-\nabla^2 - u\sum_i \delta(\mathbf{r}-\mathbf{R}_i)\right\}\psi(\mathbf{r}) = k_0^2\psi(\mathbf{r}). \tag{2.10}$$

Here $\mathbf{R}_i$ are the random positions of the scatterers, distributed according to a density $n(\mathbf{r})$.

### C. The *t* matrix of a single scatterer

We first consider the case when only one scatterer is present at position $\mathbf{r}$. The $t$ matrix of the point scatterer is simply the sum of the Born series expressing repeated scattering events at the same scatterer:

$$t(\mathbf{r}) = u + uG(\mathbf{r},\mathbf{r})u + uG(\mathbf{r},\mathbf{r})uG(\mathbf{r},\mathbf{r})u + \cdots \tag{2.11}$$

$$= \frac{u}{1-uG(\mathbf{r},\mathbf{r})}. \tag{2.12}$$

Note that since the scatterer is pointlike, there is no momentum dependence and the $t$ matrix is diagonal in real space. Equation (2.12) depends on the return Green's function $G$, which we have not expressed yet. As $G$ is a property of the (local) environment of the scatterer, it is clear what the physical significance of the $t$ matrix is *the t matrix describes the effect of a scatterer in its local environment.* In the case where many randomly positioned scatterers are present, the return Green's function $G(\mathbf{r},\mathbf{r})$ in $t$ depends on $t$ itself, which makes Eq. (2.12) self-consistent. This means the $t$ matrix is not a property that can be taken from literature. It must be calculated explicitly using the appropiate return Green's function in the system under consideration.

In one dimension (1D), Eq. (2.12) is well defined. For $d \geqslant 2$, the real part of the return Green's function diverges and a reinterpretation is needed. Indeed, for a pure system in three dimensions the divergency is well known from the equivalent of Coulomb's law,

$$G(\mathbf{r},\mathbf{r}') = \frac{e^{ik|\mathbf{r}-\mathbf{r}'|}}{4\pi|\mathbf{r}-\mathbf{r}'|} \approx \frac{1}{4\pi|\mathbf{r}-\mathbf{r}'|} + \frac{ik}{4\pi}. \tag{2.13}$$

As this divergent term appears in the denominator of (2.12), the $t$ matrix vanishes, strictly speaking. This problem was discussed for scatterers in free space in Ref. 9. We will examine this problem in more detail for constricted geometries in Sec. V.

For now, we will proceed using the simplest way around this problem, known as the second order Born approximation. This approximation is commonly used in electronic systems. Indeed, approaches with random potentials that obey Gaussian statistics are equivalent to the second order Born approximation. One of our aims is to see whether this is still a good approximation in cavities. In this approach, one has

$$t_{\mathrm{Born}} = u + iu^2 \mathrm{Im}\, G(\mathbf{r},\mathbf{r}) \approx iu^2 \mathrm{Im}\, G(\mathbf{r},\mathbf{r}). \tag{2.14}$$

The real part $u$ gives rise to a small average potential and will be neglected from here on. This approximation maintains the property of scattering, but it does not take into account possible resonant behavior of the scatterer. In general, it is a good approximation for very weak scatterers. In Sec. V, we will turn to the problem of including the full $t$ matrix in our calculations. This will give rise to interesting resonance effects near the subband edge.

### D. The amplitude Green's function and the self-energy

The self-energy $\Sigma(\mathbf{r},\mathbf{r}')$ is defined as the sum of all irreducible scattering events that may be inserted in a Green's function line. As the density of impurities is low, we can restrict ourselves to the lowest-order approximation to the average self-energy, which is diagonal in the space coordinates, $\Sigma(\mathbf{r},\mathbf{r}') = \delta(\mathbf{r}-\mathbf{r}')\Sigma(\mathbf{r})$ with

$$\Sigma(\mathbf{r}) \approx n(\boldsymbol{\rho}) t_{\mathrm{Born}}(\mathbf{r}) = iu^2 n(\boldsymbol{\rho}) \mathrm{Im} G(\mathbf{r},\mathbf{r}). \tag{2.15}$$

The average Green's function $G$ is expressed in the (average) self-energy by the Dyson equation:

$$G(\mathbf{r},\mathbf{r}') = G^0(\mathbf{r},\mathbf{r}') + \int d^3\mathbf{r}'' G^0(\mathbf{r},\mathbf{r}'')\Sigma(\mathbf{r}'')G(\mathbf{r}'',\mathbf{r}'). \tag{2.16}$$

To deal with the multiple scattering problem, we have to average over impurity positions, weighted with their density $n(\boldsymbol{\rho})$. Within the second order Born approximation, we find an explicit form for the Green's functions $G_{\mathbf{p}}$ of the mode $\mathbf{p}$,

$$G_{\mathbf{p}}(q) = \frac{1}{\mathbf{p}^2 + q^2 - k_0^2 - \Sigma_{\mathbf{p}}}. \tag{2.17}$$

In the second order Born approximation $\Sigma_{\mathbf{p}} = i\Gamma_{\mathbf{p}}$, so the resonance width reads

$$\begin{aligned}\Gamma\mathbf{p} &= \int d^2\boldsymbol{\rho} n(\boldsymbol{\rho}) \mathrm{Im} t_{\mathrm{Born}}(\boldsymbol{\rho}) \Psi_{\mathbf{p}}^2(\boldsymbol{\rho}) \\ &= \int d^2\boldsymbol{\rho} u^2 n(\boldsymbol{\rho}) \mathrm{Im}\, G(\boldsymbol{\rho},z,\boldsymbol{\rho},z) \Psi_{\mathbf{p}}^2(\boldsymbol{\rho}) \\ &= \int d^2\boldsymbol{\rho} u^2 n(\boldsymbol{\rho}) \sum_{\mathbf{p}'} \mathrm{Im} G_{\mathbf{p}'}(z,z) \Psi_{\mathbf{p}'}^2(\boldsymbol{\rho}) \Psi_{\mathbf{p}}^2(\boldsymbol{\rho}).\end{aligned} \tag{2.18}$$

The result for $\Gamma_{\mathbf{p}}$ does not depend on $z$, since after averaging we have translational invariance when we are far away from the leads at $z=0$ and $z=d_z$. The form (2.17) for $G$ yields in real space

$$\begin{aligned}G_{\mathbf{p}}(z,z') &= \frac{i\exp\{i\sqrt{k_0^2-\mathbf{p}^2+i\Gamma_{\mathbf{p}}}|z-z'|\}}{2\sqrt{k_0^2-\mathbf{p}^2+i\Gamma_{\mathbf{p}}}} \\ &= \frac{ie^{iq_{\mathbf{p}}|z-z'|}}{2q_{\mathbf{p}}+i/l_{\mathbf{p}}} e^{-|z-z'|/2l_{\mathbf{p}}},\end{aligned} \tag{2.19}$$

with

$$q_{\mathbf{p}} = \mathrm{Re}\sqrt{k_0^2-\mathbf{p}^2+i\Gamma_{\mathbf{p}}} \tag{2.20}$$

and

$$l_{\mathbf{p}} = \frac{1}{2\,\mathrm{Im}\sqrt{k_0^2-\mathbf{p}^2+i\Gamma_{\mathbf{p}}}}. \tag{2.21}$$

The quantity $l_{\mathbf{p}}$ is the mode-dependent elastic mean free path. We find the self-consistent equation

$$\Gamma_{\mathbf{p}}=\Gamma_{\mathbf{p}}^{D}, \tag{2.22}$$

$$\Gamma_{\mathbf{p}}^{D}\equiv\sum_{\mathbf{p}'} N_{\mathbf{pp}'}\nu_{\mathbf{p}'}, \tag{2.23}$$

$$\nu_{\mathbf{p}}(k_0)\equiv\mathrm{Re}\ \frac{1}{2\sqrt{k_0^2-\mathbf{p}^2+i\Gamma_{\mathbf{p}}}}=\frac{\frac{1}{2}q_{\mathbf{p}}}{|k_0^2-\mathbf{p}^2+i\Gamma_{\mathbf{p}}|}, \tag{2.24}$$

$$N_{\mathbf{pp}'}\equiv u^2\int d^2\boldsymbol{\rho}\, n(\boldsymbol{\rho})\Psi_{\mathbf{p}}^2(\boldsymbol{\rho})\Psi_{\mathbf{p}'}^2(\boldsymbol{\rho}). \tag{2.25}$$

The number of states (per unit length) in a mode $\mathcal{N}_{\mathbf{p}}$ is

$$\mathcal{N}_{\mathbf{p}}=\frac{1}{\pi}\mathrm{Re}\sqrt{k_0^2-\mathbf{p}^2+i\Gamma_{\mathbf{p}}}, \tag{2.26}$$

from which we can see that $\nu_{\mathbf{p}}$ is proportional to the density of states

$$\nu_{\mathbf{p}}=\frac{\pi}{2k_0}\frac{d\mathcal{N}_{\mathbf{p}}}{dk_0}. \tag{2.27}$$

### E. The Bethe-Salpeter equation

To describe transport of intensity, electromagnetic energy, or the probability of Schrödinger's particles through the system, we need the averaged intensity Green's function,

$$H(\mathbf{r},\mathbf{r}')=\overline{G(\mathbf{r},\mathbf{r}')G^*(\mathbf{r},\mathbf{r}')}. \tag{2.28}$$

In our model of discrete eigenmodes, we consider the projection of the intensity Green's function $H_{\mathbf{pp}'}$. It describes the propagation of *intensity* from mode $\mathbf{p}$ to $\mathbf{p}'$, and it obeys the following Bethe-Salpeter (BS) equation:

$$\begin{aligned}H_{\mathbf{pp}'}(z,z')&=G_{\mathbf{p}}(z,z')G_{\mathbf{p}}^*(z,z')\delta_{\mathbf{pp}'}\\&\quad+\sum_{\mathbf{p}''}\int dz''G_{\mathbf{p}}(z',z'')G_{\mathbf{p}}^*(z',z'')\\&\quad\times U_{\mathbf{pp}''}H_{\mathbf{p}''\mathbf{p}'}(z'',z').\end{aligned} \tag{2.29}$$

This equation involves the irreducible vertex $U_{\mathbf{pp}'}$. In our situation, it is independent of $z$ for $0<z<d_z$, while it vanishes in the leads $-\infty<z<0$ and $d_z<z<\infty$. The irreducible vertex can be shown to be the sum of all two-particle irreducible diagrams that can be inserted in the *intensity* Green's function. Two-particle irreducible in this context means that the diagrams cannot be split into two separate diagrams by cutting one propagator and one complex conjugated propagator line.

The irreducible vertex is not available in a closed form, so it must be approximated. We are however, *not* free in choosing how to approximate it: the approximation must be consistent with the approximation to $\Sigma$ that we made earlier. This can be understood as follows: $U$ describes the emission of diffuse intensity by the scatterers, $\Sigma$ describes the intensity extinction due to the scattering. If the two are not balanced, our description of the system will show *gain* or *absorbtion*, which is certainly unphysical in the systems we consider here. Flux conservation is guaranteed by the Ward-Takahashi identity, which can be derived from field theory or by manipulation of diagrams.[10,11]

$$\mathrm{Im}\Sigma_{\mathbf{p}}^{D}=\sum_{\mathbf{p}'} U_{\mathbf{pp}'}\mathrm{Im}\, G_{\mathbf{p}'}(z,z). \tag{2.30}$$

If this identity holds, flux is conserved to every order in the scatterer density, while most of our other approximations are valid only in leading order in density. Comparing (2.30) to (2.22) shows that

$$U_{\mathbf{pp}'}=N_{\mathbf{pp}'} \tag{2.31}$$

satisfies the Ward-Takahashi identity. It is, in fact, the ladder vertex, constituting one step in a ladder diagram. It is known from transport theory that the ladder diagrams describe diffusive transport.

### F. Solving the transport equation in a waveguide

Since we cannot solve the BS equation analytically, we will try to gain as much information as possible from approximations. The quantities we are interested in are the average longitudinal intensity transmission coefficients $T_{\mathbf{ab}}$, where we use $\mathbf{a}$ for the transverse momentum of an incoming cavity mode and $\mathbf{b}$ for an outgoing mode.

We consider a wave coming in from $z=-\infty$ of the form $\psi_{\mathrm{in}}(\mathbf{r})=\Psi_{\mathbf{a}}(\boldsymbol{\rho})\exp(iq_{\mathbf{a}}z)$. It will be attenuated upon entering the disordered region. This is described by the amplitude Green's function. In the disordered section, it gives rise to a source intensity

$$S_{\mathbf{p}}(z)=\delta_{\mathbf{p},\mathbf{a}}e^{-z/l_{\mathbf{p}}}. \tag{2.32}$$

We have neglected possible surface reflections as we assume the dispersion relation to be the same inside the disordered region as outside. The total intensity present in any mode as a function of position is denoted $\Phi_{\mathbf{p}}(z)$. Using (2.29), it can be shown that this quantity obeys the ladder equation

$$\Phi_{\mathbf{p}}(z)=S_{\mathbf{p}}+\int_0^{d_z}dz'G_{\mathbf{p}}(z,z')G_{\mathbf{p}}^*(z,z')\sum_{\mathbf{p}'} U_{\mathbf{pp}'}\Phi_{\mathbf{p}'}(z'). \tag{2.33}$$

We can reexpress this by expanding the Green's functions

$$\Phi_{\mathbf{p}}(z)=S_{\mathbf{p}}(z)+\frac{\nu_{\mathbf{p}}}{2\Gamma_{\mathbf{p}}l_{\mathbf{p}}}\int_0^{d_z}dz'e^{-|z-z'|/l_{\mathbf{p}}}\sum_{\mathbf{p}'} U_{\mathbf{pp}'}\Phi_{\mathbf{p}'}(z'), \tag{2.34}$$

where we have inserted the relation

$$\frac{1}{|k_0^2-\mathbf{p}^2+i\Gamma_{\mathbf{p}}|}=\frac{2\nu_{\mathbf{p}}}{\Gamma_{\mathbf{p}}l_{\mathbf{p}}}.$$

Equation (2.34) is a linear system of Fredholm integral equations of the second kind. The solution of this type of equation, for $d_z\to\infty$, is the sum of a homogeneous solution, $\Phi^H$, and a special solution $\Phi^{\mathbf{a}}$, which is dependent on the source term $S_{\mathbf{a}}$. (In fact, the special solution is defined, ex-

cept for a multiple of the homogeneous solution which we can add to it. We will choose $\Phi^{\mathbf{a}}$, such that it remains finite as $z\to\infty$.)

By differentiating the system of Fredholm equations, we find the following equivalent set of differential equations:

$$\Phi''_{\mathbf{p}}(z)=\frac{1}{l_{\mathbf{p}}^2}\Phi_{\mathbf{p}}(z)-\frac{\nu_{\mathbf{p}}}{\Gamma_{\mathbf{p}}l_{\mathbf{p}}^2}\sum_{\mathbf{p}'}U_{\mathbf{pp}'}\Phi_{\mathbf{p}'}(z), \tag{2.35}$$

$$l_{\mathbf{p}}\Phi'_{\mathbf{p}}(0)=-2S_{\mathbf{p}}(0)-\Phi_{\mathbf{p}}(0), \tag{2.36}$$

$$l_{\mathbf{p}}\Phi'_{\mathbf{p}}(d_z)=\Phi_{\mathbf{p}}(d_z). \tag{2.37}$$

We will first study the solution to the homogeneous form of the system (2.35), that is to say, we take $S=0$ and $d_z\to\infty$. Then, we have only the boundary condition (2.36) at $z=0$. This will then be used to construct a solution for finite $d_z$.

Using Eq. (2.23), the Ward identity (2.30) can be written as

$$\sum_{\mathbf{p}'}U_{\mathbf{pp}'}\nu_{\mathbf{p}'}=\Gamma_{\mathbf{p}}. \tag{2.38}$$

This implies that the right hand side of Eq. (2.35) vanishes if we insert $\Phi_{\mathbf{p}}(z)\propto\nu_{\mathbf{p}}$. The differential equation, therefore, has a solution of the form

$$\Phi_{\mathbf{p}}^H(z)=(z_0+z)\nu_{\mathbf{p}}\quad\text{for}\quad z\gg l_{\mathbf{p}}. \tag{2.39}$$

Near the boundary, there will be other terms because of the condition (2.36). They are related to the nonzero eigenvalues of the matrix, so they decay exponentially away from the edges. The asymptotic behavior of the homogeneous solution is characteristic of one-dimensional diffusion: the intensity decreases linearly with $z$. As expressed by the factor $\nu_{\mathbf{p}}$ in (2.39), the intensity is distributed over the modes according to their density of states. The shift $z_0$ will be calculated further on, when we take into account the boundaries.

The special solution for an incoming wave of unit intensity, $\psi^{\text{in}}=e^{iq_zz}\Psi_{\mathbf{a}}$ in mode $\mathbf{a}$ is called $\Phi^{\mathbf{a}}$. In the case of a semi-infinite system, we can choose it such that it converges to a constant away from the boundary. The distribution over the modes is then given by

$$\Phi_{\mathbf{p}}^{\mathbf{a}}(z)\to C_{\mathbf{a}}\nu_{\mathbf{p}},\quad z\gg l_{\mathbf{p}}. \tag{2.40}$$

The coefficient $C_{\mathbf{a}}$ is different for each incoming mode.

We now examine the behavior of the solutions to (2.35) in terms of the eigenvalues of the matrix of the system. There are exponentially growing solutions, exponentially decaying ones, and linear+constant solutions corresponding to the zero eigenvalue of the system. For a semi-infinite system, the exponentially growing solutions will be absent. The equation can then be solved formally, yielding

$$\Phi_{\mathbf{p}}(z)=\sum_i c_iR_{\mathbf{p}}^ie^{-z\lambda_i}+(\alpha+\beta z)R_{\mathbf{p}}^0, \tag{2.41}$$

where $R_{\mathbf{p}}^i$ are the right eigenvectors of the system (2.39) and all eigenvalues $\lambda_i$ are positive. The linear plus constant term corresponds to the eigenvalue zero of the system, with the right-eigenvector $R_{\mathbf{p}}^0=\nu_{\mathbf{p}}$.

The boundary condition at $z=0$ puts constraints on the coefficients $\alpha$, $\beta$, and $c_i$. For the homogeneous solution defined in (2.39), the boundary condition is

$$l_{\mathbf{p}}\Phi'_{\mathbf{p}}(0)=\Phi_{\mathbf{p}}(0). \tag{2.42}$$

According to this definition, $\beta=1$ and $\alpha=z_0$, which leads to the equation for the coefficients of the homogeneous solution $c_i^H$:

$$\sum_i c_i^Hr_{\mathbf{p}}^i(\lambda_il_{\mathbf{p}}+1)+z_0R_{\mathbf{p}}^0=R_{\mathbf{p}}^0l_{\mathbf{p}}. \tag{2.43}$$

For the special solution to the problem of a source intensity in channel $\mathbf{a}$, the definition (2.40) leads to $\alpha=C_{\mathbf{a}}$ and $\beta=0$. The resulting equation for the coefficients $c_i^{\mathbf{a}}$ of the special solution reads

$$\sum_i c_i^{\mathbf{a}}R_{\mathbf{p}}^i(\lambda_il_{\mathbf{p}}+1)+C_{\mathbf{a}}R_{\mathbf{p}}^0=2\delta_{\mathbf{a},\mathbf{p}}. \tag{2.44}$$

This equation is very similar to (2.43), if we take the sum $\Sigma_{\mathbf{a}}R_{\mathbf{a}}^0l_{\mathbf{a}}\cdots$ on both sides of (2.44), the equations become identical and we can conclude

$$z_0=\frac{1}{2}\sum_{\mathbf{a}}\nu_{\mathbf{a}}l_{\mathbf{a}}C_{\mathbf{a}}. \tag{2.45}$$

A very useful sum rule can be found from this equation by multiplying (2.44) by $R_{\mathbf{a}}^0$ on both sides and summing:

$$\sum_{i,\mathbf{a}}R_{\mathbf{a}}^0c_i^{\mathbf{a}}R_{\mathbf{p}}^i(\lambda_il_{\mathbf{p}}+1)+R_{\mathbf{a}}^0C_{\mathbf{a}}R_{\mathbf{p}}^0=2R_{\mathbf{p}}^0. \tag{2.46}$$

Taking the inproduct with a vector orthogonal to the leftmost term, but not to $R_{\mathbf{p}}^0$, we find

$$\sum_{\mathbf{a}}\nu_{\mathbf{a}}C_{\mathbf{a}}=2. \tag{2.47}$$

To find another useful constant, we study the two-particle Green's function $H$. From the time reversal symmetry of the problem, we can derive an useful identity:

$$H_{\mathbf{pp}'}(z,z')=H_{\mathbf{p}'\mathbf{p}}(z',z). \tag{2.48}$$

If we let $z'$ become large, the Green's function will behave like the homogeneous solution $\Phi^H$ near $z=0$, because all other contributions are extinguished within a few mean free paths from $z'$. From the symmetry property (2.48) and the behavior at large $z$, we find the mode distribution at $z'$ must be proportional to $\nu_{\mathbf{p}}$:

$$\lim_{z'\to\infty}H_{\mathbf{pp}'}(z,z')=C_0\nu_{\mathbf{p}'}\Phi_{\mathbf{p}}^H(z). \tag{2.49}$$

To find an expression for the coefficient $C_0$, we consider a point source in mode $\mathbf{a}$ at a large distance $z_1\gg l$ from the boundary, so that all contributions that correspond to the nonzero eigenvalues of the system will have damped out there. It follows that we only have to consider the contribution that corresponds to the zero eigenvalue, which yields, by considering the jump in the derivative,

$$C_0=\left\{\sum_{\mathbf{p}} \nu_{\mathbf{p}} l_{\mathbf{p}} \Gamma_{\mathbf{p}}\right\}^{-1}. \tag{2.50}$$

Using this coefficient, we find an expression for $C_{\mathbf{p}}$:

$$C_{\mathbf{p}}=\int_0^{\infty} dz e^{-z/l_{\mathbf{p}}} C_0 \sum_{\mathbf{p}'} U_{\mathbf{pp}'} \Phi^H_{\mathbf{p}'}(z), \tag{2.51}$$

leading to the interesting relation

$$\Phi^H_{\mathbf{p}}(0)=\frac{\nu_{\mathbf{p}}}{2\Gamma_{\mathbf{p}} l_{\mathbf{p}} C^0} C_{\mathbf{p}}. \tag{2.52}$$

### G. Transmission coefficients

If the sample is finite, a certain fraction of the intensity that enters the sample at $z=0$ will be transmitted to $z=d_z$. We can calculate the transmission coefficients from channel **a** to channel **b** for optically thick samples (length of many mean free paths) by matching the solution of the ladder equation near both boundaries:

(i) For $z \geqslant 0$, but $z-d_z \gg l_{\mathbf{p}}$, the solution will be the sum of the special solution and a multiple of the homogeneous solution

$$\Phi_{\mathbf{p}}(z)=-c\Phi^H_{\mathbf{p}}(z)+\sum_{\mathbf{p}'} \int_0^{\infty} dz' H_{\mathbf{pp}'}(z,z') U_{\mathbf{p}'\mathbf{a}} e^{-z'/l_{\mathbf{a}}}. \tag{2.53}$$

(ii) For $z \leqslant d_z$, but $z \gg l_{\mathbf{p}}$, the problem can be considered from $z=L$. There is no incoming intensity and only the homogeneous solution will be present,

$$\Phi_{\mathbf{p}}(z)=c\Phi^H_{\mathbf{p}}(d_z-z). \tag{2.54}$$

In the bulk, both solutions have a linear+constant form. This makes it possible to match a (special+homogeneous) solution at $z=0$ to a (homogeneous) solution at $z=d_z$

$$\Phi^{\text{bulk}}_{\mathbf{p}}(z)=[C_{\mathbf{a}}-c(z+z_0)]\nu_{\mathbf{p}}, \tag{2.55}$$

$$\Phi^{\text{bulk}}_{\mathbf{p}}(z)=c(d_z-z+z_0)\nu_{\mathbf{p}}. \tag{2.56}$$

It follows that

$$c=\frac{1}{(d_z+2z_0)} C_{\mathbf{a}}. \tag{2.57}$$

Since the average Green's function extinguishes in few mean free paths, we do not have to take into account the precise behavior of the intensity at $z=0$ for calculating the transmission to $z=d_z$. As usual, since the sample's length is many mean free paths, the transmitted fraction of the unscattered intensity is negligible. The intensity transmission coefficient for transmission from channel $a$ to channel $b$ is then equal to the intensity $\Phi_{\mathbf{b}}(d_z)$,

$$T_{\mathbf{ab}}=\int_0^{d_z} dz G_{\mathbf{b}}(z,d_z) G^*_{\mathbf{b}}(z,d_z) \sum_{\mathbf{p}} U_{\mathbf{bp}} \Phi_{\mathbf{p}}(z)$$

$$\approx \frac{C_{\mathbf{a}}}{(d_z+2z_0)} \Phi^H_{\mathbf{b}}(0)=\frac{C_{\mathbf{a}} C_{\mathbf{b}}}{4(d_z+2z_0) q^2_{\mathbf{b}}} \sum_{\mathbf{p}} \Gamma_{\mathbf{p}} l^2_{\mathbf{p}} \nu_{\mathbf{p}}.$$

We have now derived formula (4) of Ref. 4. It holds for the transmission of scalar waves through waveguides and can mutatis mutandis be applied to the propagation of EM waves or Schrödinger waves. Below it is used to calculate the conductance of a quantum wire.

## III. CONDUCTANCE OF ELECTRONIC SYSTEMS

We now apply our result to the electronic case of a disordered conducting channel. The Landauer formula gives the average zero temperature conductance of a sample of arbitrary dimensions connected to two reservoirs of electrons, in terms of the average flux transmission coefficients:

$$R^{-1}=G=\frac{2e^2}{h}\sum_{a,b} \mathcal{T}^{\text{flux}}_{ab}=\frac{2e^2}{h}\sum_{a,b} \frac{q_b}{q_a} T_{ab}, \tag{3.1}$$

where $2e^2/h$ is the quantum of conduction, the factor 2 comes from spin degeneracy. The flux transmission coefficients differ in our case from the intensity transmission coefficients by a factor $q_{b;0}/q_{a;0}$, where the $q_0$'s stand for the $z$-wave numbers of the incoming and outgoing waves outside the disordered region. To a good approximation, it holds for the propagating modes,

$$q_{\mathbf{a};0} \approx \sqrt{q^2_{\mathbf{a}}+l^{-2}_{\mathbf{a}}} \approx \frac{1}{2\nu_{\mathbf{a}}}. \tag{3.2}$$

With these approximations and relation (2.47), we find

$$G=\frac{2e^2}{h}\frac{4}{(d_z+2z_0)}\sum_{\mathbf{p}} \Gamma_{\mathbf{p}} l^2_{\mathbf{p}} \nu_{\mathbf{p}}. \tag{3.3}$$

From this formula, it is easy to see that Ohm's law is valid for the average conductance of samples in the semiballistic regime. The resistance, defined as the inverse of the average conductance, reads[12]

$$R=\frac{d_z}{d_x d_y}\frac{1}{\sigma}+2R_c, \tag{3.4}$$

with the conductivity

$$\sigma=\frac{8e^2}{h d_x d_y}\sum_{\mathbf{p}} \Gamma_{\mathbf{p}} l^2_{\mathbf{p}} \nu_{\mathbf{p}} \tag{3.5}$$

and the contact resistances at $z=0$ and $z=d_z$,

$$R_c=\frac{z_0}{\sigma}. \tag{3.6}$$

Note, however, that $R_c$ as well as $\sigma$ are complicated functions of $k_0$.

In Ref. 4, an analytic result was obtained for the conductance in a 2D film, with the width $d_y \to \infty$, in the limit of weak disorder:

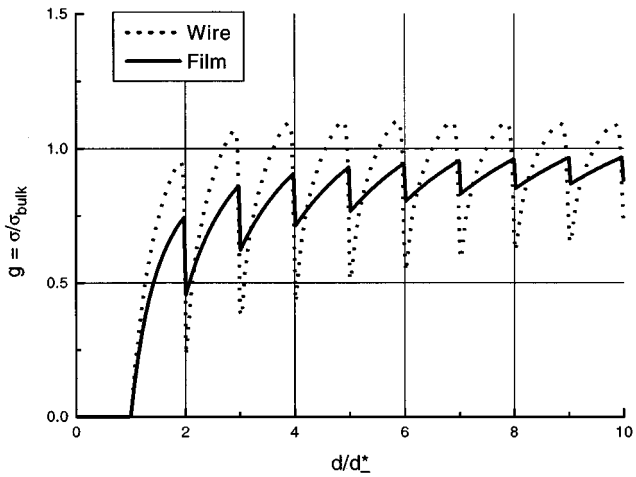


FIG. 2. Conductivities of semiballistic devices with very low disorder, in the second order Born approximation. The solid line represents the conductivity of a disordered film of width $d$ as it goes through multiples of the resonant width $d^*$. The dashed line gives the conductivity of a 1D constriction of a 2D electron gas as a function of the width $d$.

$$\frac{\sigma(d_x)}{\sigma_{\text{bulk}}}=\frac{3N}{2N+1}-\frac{1}{2}N(N+1)\frac{(d^*)^2}{d_x^2}, \tag{3.7}$$

where $d^*=\pi/k_0$ is the resonant width, $N$ is the number of open channels, and $\sigma_{\text{bulk}}=(2e^2/3\pi h)k_f^2 l_{\text{bulk}}$ is the Drude conductivity of a 3D bulk sample. This result is reproduced here in Fig. 2, together with the result for a 1D quantum wire. Both curves have been scaled with the bulk conductivity.

It is seen that these curves exhibit remarkable drops in the conductivity whenever a new cavity mode becomes resonant. These drops are explained mathematically by the density of states that grows large near the subband bottom, thus causing the second order Born $t$ matrix to become larger. This expresses more efficient scattering and, therefore, less conductance. The physical explanation is that when the new mode is not yet resonant, it does not yet contribute to conduction. There is scattering to this mode however, and the scattered waves interfere destructively with the waves present in the other modes. In Sec. V, we will study the analog of this effect for the full $t$ matrix of the point scatterers.

A different approach for calculating the conductivity was followed by Surke and Wilke in Ref. 13. These authors calculate the conductivity directly from the Kubo formula and derive expressions different from ours. Their results involve the average scattering time, rather than the inverse of the average scattering rate ($\Gamma_{\mathbf{p}}$ in our work). It therefore seems to us, that the latter results are unphysical. Indeed, one can consider cases where the scatterer density goes to zero locally, such that the average scattering time diverges. Then the resulting prediction for the conductivity diverges, while our result (3.5) is quite insensitive to such limits, as it should be.

## IV. TRANSPORT THROUGH A DOUBLE-BARRIER STRUCTURE

In Sec. II, transmission coefficients were derived for transport of wave intensity along the length of a waveguide.

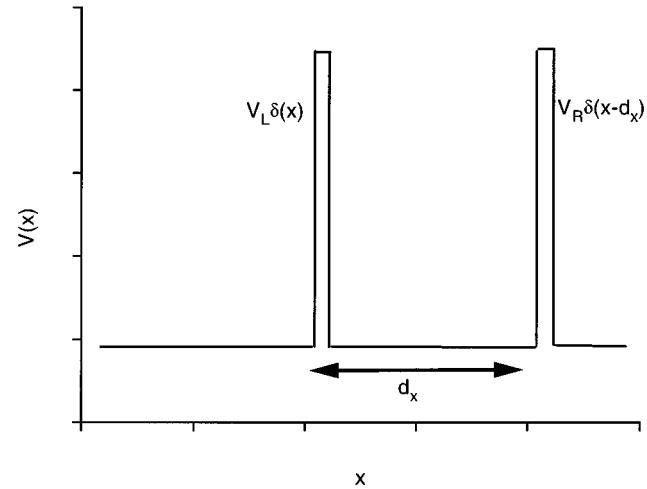


FIG. 3. A double-barrier quantum well, or its optical analogon, the Fabri Perot Interferometer, is modeled by a pair of $\delta$-function potential barriers in the $x=0$ and $x=d_x$ planes. Between these mirrors, impurities are present. Transport occurs in the $x$ direction, tunneling through the barriers.

In some systems, like the Fabry-Perot Interferometer (FPI), or its electronical analog, the double-barrier quantum well (DBQW), transport occurs in the transversal direction, due to ''tunneling'' through the barriers.

In the absence of random scattering, these devices transmit only waves for which the perpendicular component of the wave vector is resonant with the cavity. The linewidth is very small, usually the $Q$ factor of these devices is several thousands. The pure FPI transmits a light beam that meets the resonance condition without changing its direction.

The devices we are interested in contain a small density of impurities, such that the width $d_x$ of the device is still much smaller than the mean free path, but the width multiplied by the $Q$ factor is much larger than the mean free path. The problem of multiple scattering in such devices was first considered on a fundamental level by Berkovits and Feng.[14] Their approach is valid for the situation of one resonant mode, well away from the onset of further cavity resonances.

The behavior near resonances in the multimode situation was later discussed by one of us.[4] In the present section, we will discuss the derivation of these results. It will be seen that multiple elastic scattering will broaden the resonance linewidth and cause transmission of the energy into all available outgoing channels, independent of the incoming channel.

### A. Double-barrier system in one dimension

First, for simplicity, we will consider a one-dimensional DBQW like in Fig. 3, with the potential between the barriers equal to that outside. We will describe these barriers, which are imperfect mirrors, by strong $\delta$-function potentials. Their strengths are allowed to have an imaginary part to model absorbtion of waves by the mirrors

$$V(x)=V_L\delta(x)+V_R\delta(x-d_x). \tag{4.1}$$

The intensity transmission, reflection and absorbtion coefficients of the single barriers follow from requiring continuity of the wave function across the barrier:

$$T=\frac{4k_0^2}{|V+2ik_0|^2},\quad R=\frac{|V|^2}{|V+2ik_0|^2}. \tag{4.2}$$

If $V$ is purely real, there is no absorbtion and the identity $T+R=1$ holds. If $\mathrm{Im}V>0$, the model describes a barrier with nonzero absorbtion coefficient $A$:

$$A=1-R-T=\frac{4k_0\mathrm{Im}V}{|V+2ik_0|^2}. \tag{4.3}$$

A description with absorption is realistic in the optical case, where the absorbtion coefficient of a mirror may be larger than the transmission coefficient. In the electronic case, there should be no absorbtion, but there could be loss of phase coherence that can lead to similar effects.

Now we look at the Green's function inside the structure, $G(x,x')$ for $0<x,x'<d_x$. By requiring continuity at both barriers we can see it is, neglecting terms of order $1/V^2$,

$$G(x,x')=-\frac{2i}{k_0}\frac{\sin(k_0x+\delta)\sin(k_0x'+\delta)}{\sin(k_0d_x)+\dfrac{2ik_0}{V_L-2ik_0}+\dfrac{2ik_0}{V_R-2ik_0}}, \tag{4.4}$$

where $\delta$ is a (complex) phase shift that becomes small near resonances. In the ideal system ($V$ real and very large), these resonances occur when $k_0=n\pi/d_x$. If the linewidth of the structure is much smaller than the mode separation, which is the case for high-$Q$ cavities, we can make a Lorentzian approximation to the line shape and express the propagator as a sum over mode wave functions:

$$G(x,x')=\sum_{p_x=n\pi/d_x}\Psi_{p_x}(x)G_{p_x}(k_0)\Psi_{p_x}(x'), \tag{4.5}$$

involving the mode wave functions

$$\Psi_{p_x}(x)=\sqrt{\frac{2}{d_x}}\sin(p_xx+\delta_{p_x}) \tag{4.6}$$

and the mode propagator (upon neglecting small shifts of the resonance positions),

$$G_{p_x}(k_0)=\frac{1}{p_x^2-k_0^2-i\Gamma_{p_x}^{\mathrm{pure}}}. \tag{4.7}$$

The linewidth $\Gamma^{\mathrm{pure}}$ is due to absorbtion and transmission of the barriers:

$$\Gamma_{p_x}^{\mathrm{pure}}=\frac{p_x}{2d_x}(A_L+T_L+A_R+T_R), \tag{4.8}$$

where $L,R$ stands for left and right, respectively. This expression of the linewidth in terms of transmission and absorbtion coefficients is valid for general barrier potentials.

A beam coming in from $x=-\infty$ of the form $\exp(ik_0x)$, with $k_0$ close to some resonant $p_x$ will give rise to a standing wave inside the structure. The amplitude of this wave is found by matching at the boundaries, which gives, approximating for $k_0$ near $p_x$,

$$\psi(x)=\frac{-2ik_0^2}{V_L-2ik_0}\Psi_{p_x}(x)G_{p_x}\sqrt{\frac{2}{d_x}}. \tag{4.9}$$

To describe realistic situations we need to expand the simple 1D model to a three-dimensional model with barriers (mirrors) at $x=0$, $x=d_x$. There are three regimes for this generalization:

(i) A structure that is confined in both $y$ and $z$ dimensions, like a double-barrier structure inside a waveguide.

(ii) A structure that is confined in the $y$ direction, but very large in the $z$ dimension, for example, a double-barrier structure inside a 2D electron gas.

(iii) A structure that is very large in both $y$ and $z$ dimensions, like an optical FPI or a double-barrier quantum well inside a three-dimensional semiconductor sample.

The first case is the simplest to describe, we will analyze it first and then take the continuum limit in two directions. Results for the pure case follow from simply replacing the 1D mode eigenfunctions with the 3D eigenfunctions and replacing the mode energy $p_x^2$ by $\mathbf{p}^2=p_x^2+p_y^2+p_x^2$,

$$G(\mathbf{r},\mathbf{r}')=\sum_{\mathbf{p}=p_x,p_y,p_z}\Psi_{\mathbf{p}}(\mathbf{r})G_{\mathbf{p}}(k_0)\Psi_{\mathbf{p}}(\mathbf{r}'), \tag{4.10}$$

$$\Psi_{\mathbf{p}}(\mathbf{r})=\sqrt{\frac{8}{d_xd_yd_z}}\sin(xp_x)\sin(yp_y)\sin(zp_z), \tag{4.11}$$

$$G_{\mathbf{p}}(k_0)=\frac{1}{\mathbf{p}^2-k_0^2-i\Gamma_{p_x}^{W}}. \tag{4.12}$$

We can see from the diagonality of the Green function that only waves, which have a $k_x$ resonant with the structure, will be transmitted into the same $y,z$ mode of the waveguide surrounding the structure, i.e., the interferometer selectively transmits waves, it does not change their direction.

In the case where scatterers are present, there will be a self-energy $\Sigma^D$, due to disorder in addition to $i\Gamma^{\mathrm{pure}}$. One has

$$\Sigma_{\mathbf{p}}=\Sigma_{\mathbf{p}}^{\mathrm{pure}}+\Sigma_{\mathbf{p}}^{D}\approx i\Gamma_{\mathbf{p}}^{\mathrm{pure}}+\Sigma_{\mathbf{p}}^{D}. \tag{4.13}$$

We are interested in the regime where the latter has a much greater imaginary part, $\Gamma^D\gg\Gamma^{\mathrm{pure}}$. This is the case for a cavity with a very high intrinsic $Q$ factor and a low density of scatterers. Let us consider the transmission of a plane wave coming in from $x=-\infty$, with wave vector $\mathbf{a}$. (Note that, in this section, we consider transmission *through* the cavity boundaries, whereas in the previous section transmission was *within* them, therefore the incoming beam is now in the $x$ direction.) The momentum in the $y$ and $z$ directions is quantized, while the momentum in the $x$ direction outside the structure is determined by the total wave number, $a_x=\sqrt{k^2-a_y^2-a_z^2}$,

$$\Psi_{\mathrm{in}}=e^{ia_xx}\sqrt{\frac{4}{d_yd_z}}\sin(a_yy)\sin(a_zz). \tag{4.14}$$

This incoming wave gives rise to an intensity inside the structure of

$$I(\mathbf{r})=\sum_{p_x}\frac{2p_x^2}{d_x}T_{\mathbf{p}}^L|G_{\mathbf{p}}|^2|\Psi_{\mathbf{p}}(\mathbf{r})|^2\delta_{p_y,a_y}\delta_{p_z,a_z}. \tag{4.15}$$

In the case where no scatterers are present, the intensity of the transmitted wave will be

$$I_{\rm tr}=\sum_{p_x}\frac{p_x^2}{d_x^2}T_{\mathbf{p}}^L T_{\mathbf{p}}^R|G_{\mathbf{p}}|^2\delta_{p_y,a_y}\delta_{p_z,a_z}. \tag{4.16}$$

At resonance this transmission is unity for the case of symmetric, nonabsorbing barriers. In practice, only one of the modes will contribute to this transmission.

In the case when scatterers are present, intensity will build up in the cavity in essentially the same way, due to the condition $l>>d_x$, but the dominant decay of the intensity will be due to scattering to other modes. Hence, (4.15) is still valid in this case, but we must take the Green function with the disorder term $\Sigma^D$ in the self-energy. The incoming intensity will now be the source term for a BS equation, which reads

$$\Phi_{\mathbf{p}}=|G_{\mathbf{p}}|^2\left\{\frac{2p_x^2}{d_x}T_{\mathbf{p}}^L\delta_{p_y,a_y}\delta_{p_z,a_z}+\sum_{\mathbf{p}'}U_{\mathbf{pp}'}\Phi_{\mathbf{p}'}\right\}. \tag{4.17}$$

$\Phi_{\mathbf{p}}$ is the intensity in mode $\mathbf{p}$, $U_{\mathbf{pp}'}$ is the irreducible vertex. Since there are only discrete modes now, this is just a matrix inversion problem:

$$\sum_{\mathbf{p}'}\left(\delta_{\mathbf{pp}'}-\frac{\mathrm{Im}G_{\mathbf{p}}}{\Gamma_{\mathbf{p}}}U_{\mathbf{pp}'}\right)\Phi_{\mathbf{p}'}=|G_{\mathbf{p}}|^2\frac{2p_x^2}{d_x}T_{\mathbf{p}}^L\delta_{p_y,a_y}\delta_{p_z,a_z}. \tag{4.18}$$

The matrix in the brackets has one eigenvalue close to zero, which will dominate the solution. To see this, we multiply by $\Gamma_{\mathbf{p}}$ and sum over $\mathbf{p}$, using (2.30) and (4.13) to find

$$\sum_{\mathbf{p}}\Gamma_{\mathbf{p}}^{\rm pure}\Phi_{\mathbf{p}}=\sum_{\mathbf{p}}\Gamma_{\mathbf{p}}|G_{\mathbf{p}}|^2\frac{2p_x^2}{d_x}T_{\mathbf{p}}^L\delta_{p_y,a_y}\delta_{p_z,a_z}. \tag{4.19}$$

We expect the intensity in each mode to be proportional to the density of states (this approximation is very good if the scattering rate is much greater than the cavity loss rate). Also, if the incoming wave is close to one resonant mode, we can neglect contributions of the other modes. This allows us to solve (4.18) and find

$$\Phi_{\mathbf{p}}=\frac{\Gamma_{\mathbf{p}}|G_{\mathbf{p}}|^2}{\Sigma_{\mathbf{p}'}\Gamma_{\mathbf{p}'}^{\rm pure}\Gamma_{\mathbf{p}'}|G_{\mathbf{p}'}|^2}\Gamma_{\mathbf{a}}|G_{\mathbf{a}}|^2\frac{2\mathbf{a}_x^2}{d_x}T_{\mathbf{a}}^L. \tag{4.20}$$

The transmission from channel $\mathbf{a}$ to $\mathbf{b}$ is then given by

$$T_{\mathbf{ab}}=\frac{\Phi_{\mathbf{b}}}{2d_x}T_{\mathbf{b}}^R. \tag{4.21}$$

In case the double-barrier structure is large ($d_x\gg l$) and uniform in one or both of the $(x,y)$ dimensions, the sum in the denominator can be simplified, since the resonance width $\Gamma_{p_x,p_y,p_z}$ will no longer depend on the corresponding wave number. For the case where the structure is large in the $z$ dimension, we find

$$T_{\mathbf{ab}}=\frac{\mathbf{a}_x^2T_{\mathbf{a}}^L\Gamma_{\mathbf{a}}|G_{\mathbf{a}}|^2T_{\mathbf{b}}^R\Gamma_{\mathbf{b}}|G_{\mathbf{b}}|^2}{d_x^2d_z\Sigma_{p_x,p_y}\Gamma_{\mathbf{p}}^{\rm pure}\nu_{\mathbf{p}}}, \tag{4.22}$$

with the definition of $\nu_{\mathbf{p}}$ given in (2.24). This is Eq. (7) of Ref. 4. In a more restricted version with one resonant mode it was already derived in Ref. 14; note, however, that in that work the prefactor misses a factor 2.

In the case of a double-barrier structure that is much larger than the bulk mean free path in two dimensions, $(d_x,d_y\gg l)$, the denominator of (4.22) can be simplified to

$$4d_x^2d_yd_z\sum_{p_x}\Gamma_{p_x}^{\rm pure}\left(2+\frac{4}{\pi}\arctan\frac{k_0^2-p_x^2}{\Gamma_{p_x}}\right). \tag{4.23}$$

From (4.22), we see that scattering occurs into all free cavity modes. For a FPI ($d_y\to\infty$) with an incoming plane wave, scattering inside the barrier region causes an equal distribution over all directions. Therefore, the transmitted intensity does not depend on the angle of incidence in the $(y,z)$ plane. It does depend on the angle with the $x$ axis as the mode quantization implies that only certain angles are transmitted. This causes the well known appearance of fringes in the transmission pattern.

When a new cavity mode is just resonant, the return Green's function in the cavity becomes large, as is discussed in Sec. V F. This quenches scattering in the other subbands, so the device will appear less disordered. This is one of the reasons why a Fabry-Perot etalon gives the best results when used near perpendicular incidence. We should point out, however, that this effect is less pronounced for a two-dimensional structure, such as a Fabry-Pérot interferometer, than for a one-dimensional structure such as a wave guide, as the divergence of the return Green's function is only logarithmic.

### B. Electronic conductivity through a disordered double-barrier structure

In Ref. 4 results were also derived for electronic double-barrier quantum wells. The conductance of such a device is again given by the Landauer formula,

$$G=\frac{2e^2}{h}\sum_{\mathbf{ab}}\mathcal{T}_{\mathbf{ab}}. \tag{4.24}$$

In an experiment conducted by Guéret *et al.*,[8] the barriers consist of two separated layers of aluminium gallium arsenide ($Al_xGa_{1-x}As$) in a gallium arsenide (GaAs) sample. The thickness of the barriers was varied from 7.5 nm to 31 nm. Hence, the transmission coefficients, which depend exponentially on the barrier thickness, varied over nine orders of magnitude, while the width of the resonance peak remained a few mV. Elastic scattering from roughness at the interface between the GaAs and the $Al_xGa_{1-x}As$ is believed to cause this resonance broadening.

For a pure double-barrier structure, the linewidth is expected to scale linearly with the transmission coefficients:

$$\Gamma=\Gamma^W=\frac{k_0}{2d_x}(A_L+T_L+A_R+T_R). \tag{4.25}$$

The total transmission for a resonant cavity is linear in the transmission coefficients, as it is proportional to $T_LT_R\Gamma^W$.

In the case of a small amount of disorder, for a cavity at resonance, the transmission coefficients can be seen from (4.22) to be proportional to $T_LT_R\Gamma^W$, as in the pure case. The linewidth, however, is determined by $\Gamma^D$, which can be much larger. It was calculated in Ref. 4 that this multiple

scattering effect can explain the order of magnitude of the observed resonance broadening.

## V. STRONG SCATTERING: THE FULL BORN SERIES

The results of Sec. II have been derived using the second order Born approximation (2.14) to the $t$ matrix. This approximation essentially describes weak scatterers that have no *internal* resonances near the wavelength of the incident waves. Realistic systems, however, are not extremely long. If a reasonable amount of scattering is to occur, one must have moderately strong scatterers. But for such scatterers, the multiple scatterings from the walls will not at all be negligible. Rather than approximating the Born series by the first two terms, one has to sum the full series. For point scatterers in continuum space, this requires introducing either an extension of wave function space[15] or a regularization of the return Greens function. A very simple solution to this problem was given in Ref. 9. In the present section, we shall apply those ideas to cavity systems.

Scattering of Schrödinger waves in narrow systems has been studied by Bagwell.[16] He considers both finite size scatterers and point scatterers. In the latter case, the infinities that occur due to the small distance behavior are avoided by considering only a finite number of evanescent modes. As a result, the predictions of the model then depend on the number of modes considered. Chu and Sorbello[7] investigated scattering properties of finite size scatterers inside a cavity by means of the imaging method. We shall follow a different approach that is more suitable to the limit of point scatterers, and then proceed to multiple scattering situations.

### A. Point scatterer near a mirror

Boundary conditions can have a strong effect on the properties of scattering, even for point scatterers. This can already be seen from studying the following simple case: Consider a point scatterer for Schrödinger waves with bare scattering length $u$ at a (small but finite) distance $d_w$ from a perfect plane wall. This imposes the mirror boundary condition $\Psi=0$ on the surface $z=0$. The eigenfunctions of the pure system (without the scatterer) are

$$\Psi(p_x,p_y,p_z)=\sqrt{2}ie^{ip_xx}e^{ip_yy}\sin(p_zz), \tag{5.1}$$

with

$$p_x^2+p_y^2+p_z^2=k_0^2. \tag{5.2}$$

The return Green function is found by Fourier transformation:

$$G(\mathbf{r}_0,\mathbf{r}_0)=G^0(\mathbf{r}_0,\mathbf{r}_0)-G^0(\mathbf{r}_0,\mathbf{r}_0^*), \tag{5.3}$$

where $\mathbf{r}_0^*=(r_x^0,r_y^0,-r_z^0)$ is the mirror image of $\mathbf{r}_0$, and $G^0$ is the free space propagator. We distinguish a direct and a mirror term. When the distance between the scatterer and the mirror is much larger than the effective size of the scatterer, $(d_w\gg\Lambda^{-1})$, the mirror term has a regular behavior.

We then need to regularize only the direct term in (5.3), the regularized mirror term will not be much different from the unregularized form. This enables us to apply the regularization scheme in Ref. 9 to the direct term only, to find corrections due to the scattering between the impurity and its mirror image. It gives

$$G(\mathbf{r},\mathbf{r})=\frac{ik_0+\Lambda}{4\pi}-\frac{e^{2id_wk_0}}{8\pi d_w}. \tag{5.4}$$

However, when the distance between the mirror and the impurity is of the order of the effective scatterer size, this approach becomes ill behaved and we need to regularize both terms in the return Green's function. We do this by applying a regulator of the form $\Lambda^2/(\Lambda^2+p^2)$ to the Fourier integrals that are used to define the real space form of the Green's function. This regulator is well known in quantum field theory. It cuts off momenta beyond $p=\Lambda$, showing that $1/\Lambda$ is the effective size of the scatterer. In the free space situation, we thus get

$$\begin{aligned}G^0(\mathbf{r},\mathbf{r}')&=\int\frac{d^3\mathbf{p}}{(2\pi)^3}\frac{1}{\mathbf{p}^2-k_0^2-i0}\frac{\Lambda^2}{\Lambda^2+\mathbf{p}^2}e^{i\mathbf{p}\cdot(\mathbf{r}-\mathbf{r}')}\\&=\left\{\frac{e^{i|\mathbf{r}-\mathbf{r}'|k_0}}{4\pi|\mathbf{r}-\mathbf{r}'|}-\frac{e^{-|\mathbf{r}-\mathbf{r}'|\Lambda}}{4\pi|\mathbf{r}-\mathbf{r}'|}\right\}\frac{\Lambda^2}{\Lambda^2+k_0^2}.\end{aligned} \tag{5.5}$$

Now we can take the limit $\mathbf{r}'\to\mathbf{r}$. As expected, the result is finite, and reads

$$G^0(\mathbf{r},\mathbf{r})=\frac{ik_0+\Lambda}{4\pi}\frac{\Lambda^2}{\Lambda^2+k_0^2}. \tag{5.6}$$

The factor $\Lambda^2/(\Lambda^2+k_0^2)$ is near unity for scatterers that are much smaller than the wavelength. We will omit it from now on. Then (5.6) coincides with the result of Ref. 9:

$$G^0(\mathbf{r},\mathbf{r})=\frac{ik_0+\Lambda}{4\pi}. \tag{5.7}$$

The return Green's function (5.4) now reads

$$G(\mathbf{r}_0,\mathbf{r}_0)=\frac{ik_0+\Lambda}{4\pi}-\frac{e^{2ik_0d_w}-e^{-2\Lambda d_w}}{8\pi d_w} \tag{5.8}$$

and reduces to Eq. (5.4) when $\exp(-2\Lambda d_w)\ll 1$. Now we use this regularized form of the return Green's function to compute the $t$ matrix

$$t=\left[u^{-1}-\left(\frac{\Lambda+ik_0}{4\pi}-\frac{e^{2id_wk_0}-e^{-2d_w\Lambda}}{8\pi d_w}\right)\right]^{-1}. \tag{5.9}$$

Following Ref. 9 we state that by *definition*, a position dependent resonance occurs when the $t$ matrix is purely imaginary. (This need not always coincide with a sharp peak in the absolute value of the $t$ matrix.) The positions of the resonances are located at $k_0$ values, where

$$\cos(2d_wk_0)=-8\pi d_wu^{-1}+2d_w\Lambda+\exp(-2d_w\Lambda). \tag{5.10}$$

In case of Schrödinger waves, $u$ is the potential strength and does not depend on $k_0$. This implies that, for large $d_w$, there is no resonance. Indeed, in free space $(d_w=\infty)$, it is known that point scatterers for electrons do not have a resonance.

However, Eq. (5.10) shows that an infinity of resonances occur when the scatterer is attractive ($u>0$) and is located close enough to the wall.

For scatterering of scalar classical waves, the analog of the above position-dependent resonance can be found by replacing the scattering strength $u$ by $4\pi\alpha k_0^2$, where $\alpha$ is the polarizability of the point scatterer.[9] The expression for the $t$ matrix becomes

$$t=\left[\frac{1}{4\pi\alpha k_0^2}-\left(\frac{\Lambda+ik_0}{4\pi}+\frac{e^{2id_wk_0}-e^{-2d_w\Lambda}}{8\pi d_w}\right)\right]^{-1}. \tag{5.11}$$

It has resonances at

$$\cos(2d_wk_0)=2d_w\left(\frac{1}{\alpha k_0^2}-\Lambda\right)+e^{-2d_w\Lambda}. \tag{5.12}$$

For $d_w\to\infty$, this yields the resonance condition $k_0^2=k_*^2\equiv 1/\Lambda\alpha$ of Ref. 9. For large but finite $d_w$, many resonances may occur.

### B. Point scatterer in a waveguide

Next, consider a scatterer in an infinitely long channel. The Green's function for the clean channel is calculated in (2.5). It is expressed as a sum of mode propagators,

$$G(\mathbf{r},\mathbf{r}')=\sum_{\mathbf{p}}\Psi_{\mathbf{p}}(\boldsymbol{\rho})G_{\mathbf{p}}(z-z')\Psi_{\mathbf{p}}(\boldsymbol{\rho}'). \tag{5.13}$$

The mode quantum numbers $p_x,p_y$ are the discrete transversal wave numbers. For systems on a lattice, the sum over $\mathbf{p}$ converges as the distance between adjacent lattice points is a natural cutoff.

Even in a confined geometry of continuum space, we have the problem that the real part of the return Green's function diverges. In Eq. (5.13) this occurs since for large $|\mathbf{p}|$ the terms in the infinite series tend to zero as $1/p$, leading again to a linear divergency of the sum. In order to define the $t$ matrix of the point scatterer in a meaningful way, we thus still need to regularize the return Green's function.

The approach followed by Bagwell[16] is to take into account only a finite number of evanescent modes in Eq. (5.13). As the cutoff has not been related to physical properties of the scatterer, this approach is a bit unsatisfactory and unnatural.

We can regularize the sum (5.13) term by term in a way similar to (5.5), using the cutoff function $\Lambda^2/(\Lambda^2+\mathbf{p}^2+q^2)$, where $\mathbf{p}$ is now the discrete transversal wave number and where $q$ is the continuous wave number in the $z$ direction

$$G_{\mathbf{p}}(z,z')=\int_{-\infty}^{\infty}\frac{dq}{2\pi}\frac{1}{q^2+\mathbf{p}^2-k_0^2-\Sigma_{\mathbf{p}}}\frac{\Lambda^2}{\Lambda^2+\mathbf{p}^2+q^2}e^{iq(z-z')} \tag{5.14}$$

$$=\left(\frac{ie^{i\sqrt{k_0^2-\mathbf{p}^2+\Sigma_{\mathbf{p}}}|z-z'|}}{2\sqrt{k_0^2-\mathbf{p}^2+\Sigma_{\mathbf{p}}}}-\frac{e^{-\sqrt{\Lambda^2+\mathbf{p}^2}|z-z'|}}{2\sqrt{\Lambda^2+\mathbf{p}^2}}\right)\times\frac{\Lambda^2}{\Lambda^2+k_0^2+\Sigma_{\mathbf{p}}}. \tag{5.15}$$

We will consider the real space case again, omitting the factor $\Lambda^2/(\Lambda^2+k_0^2+\Sigma_{\mathbf{p}})$ from now on. The return Green's function will then be given by

$$G(\mathbf{r},\mathbf{r})=\sum_{\mathbf{p}}\Psi_{\mathbf{p}}^2(\boldsymbol{\rho})\left(\frac{1}{2\sqrt{\mathbf{p}^2-k_0^2-\Sigma_{\mathbf{p}}}}-\frac{1}{2\sqrt{\Lambda^2+\mathbf{p}^2}}\right). \tag{5.16}$$

For large $|\mathbf{p}|$, the summand is of order $p^{-3}$, so the series (5.13) converges.

For the special case where the energy $k_0^2$ approaches one of the subband bottoms $p^2$, the series contains one divergent term. As we shall see in detail below, this divergency will be regularized when the system is finite and there is conductive behavior near the boundaries.

The $t$ matrix of the point scatterer (in a channel without further randomness) now reads

$$t=\left[u^{-1}-\sum_{\mathbf{p}}\Psi_{\mathbf{p}}^2(\boldsymbol{\rho})\left(\frac{1}{2\sqrt{\mathbf{p}^2-k_0^2-\Sigma_{\mathbf{p}}}}-\frac{1}{2\sqrt{\Lambda^2+\mathbf{p}^2}}\right)\right]^{-1}. \tag{5.17}$$

If the scatterer strength is positive, that is to say, for an *attractive* scatterer potential, the $t$ matrix can have a pole. It occurs before the onset of conduction modes, thus for $k_0<|\mathbf{p}_0|$, where $\mathbf{p}_0$ is the label of the first mode. This bound state will have an energy between $0<k_0^2<\mathbf{p}_0^2$, the energy of the first subband bottom, provided that

$$0<u<\left[\sum_{\mathbf{p}}\Psi_{\mathbf{p}}^2(\boldsymbol{\rho})\left(\frac{1}{2\sqrt{\mathbf{p}^2-\Sigma_{\mathbf{p}}}}-\frac{1}{2\sqrt{\Lambda^2+\mathbf{p}^2}}\right)\right]^{-1}. \tag{5.18}$$

Thus, the bound state already occurs for rather weak scatterers, which is an indication of the failure of low-order approximations, such as the second order Born approximation. On the other hand, a *strong* attractive scatterer will have its bound state at negative energy, $E=k_0^2<0$. In an optical situation, such a state has no meaning. In an electronic system it may occur, however. If the Fermi energy is above the bound state energy, the state will always be occupied and it will not contribute to conductance. Due to the divergency of the return Green's function at the bottom of the first subband, the bound state will always occur below the first subband bottom. The weaker the scatterer is, the closer the bound state energy will move towards the first subband bottom. Also note the explicit depencence on the transversal $(x,y)$ position of the scatterer. For very weak scatterers, however, the resonance will be indistinguishable from the subband resonance and the second order Born approximation will yield good results.

### C. Resonant tunneling

Unexpected peaks have been observed in the transmission of quantum dots, narrow constrictions of a 2D electron gas.[17] Before any of the channels of the dots were open, transmission peaks of order unity were observed. They were attributed to tunneling through a bound state of a single impurity located (by accident) in the channel. We model such a narrow junction between two broad reservoirs, where conduction takes place by an infinite channel. We assume that the electrostatic potential equals $V_0$ for $0<z<L$ and van-

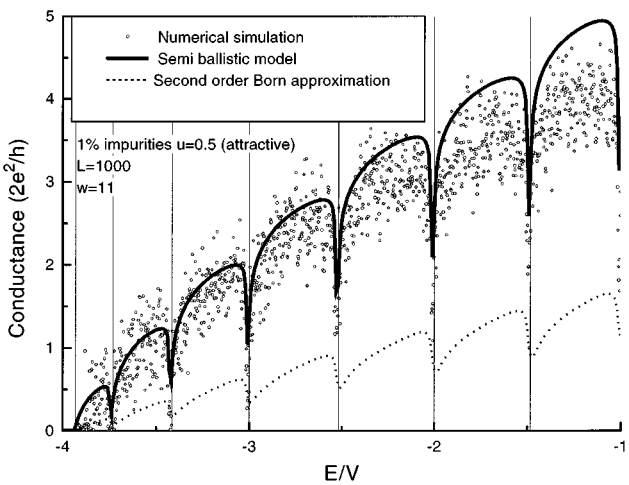


FIG. 4. Conductance of a long quantum wire containing a small density of strong attractive scatterers as a function of carrier energy $E/V$. The vertical lines indicate positions of the subband edges in the band structure of the lattice.

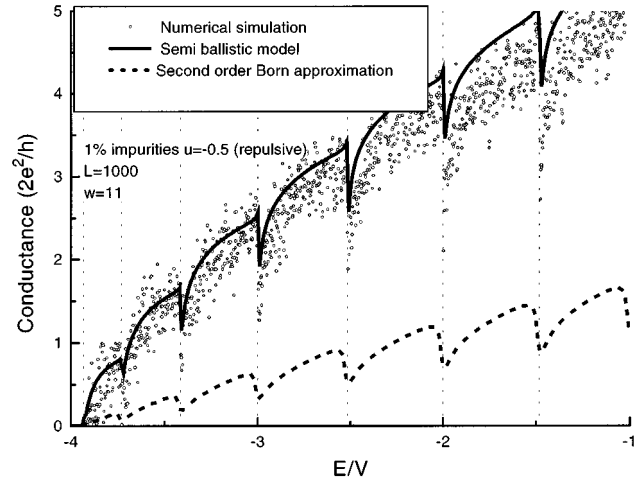


FIG. 5. Conductance of a long quantum wire containing a small density of strong repulsive scatterers as a function of carrier energy. The vertical lines indicate positions of the subband edges in the band structure of the lattice.

ishes elsewhere. This implies that for $z<0$ and for $z>L$ conduction occurs, while the junction $0<z<L$ acts as a barrier as long as $k_0^2<V_0$.

In the true 1D case, this problem can easily be solved exactly, yielding the amplitude transmission coefficient,

$$\zeta=\frac{8ik_0\kappa^2e^{-\kappa L}}{(2\kappa-u)(k_0+i\kappa)^2-uV_0[e^{-2\kappa Z_0}+e^{-2\kappa(L-Z_0)}]+(2\kappa+u)(k_0-i\kappa)^2e^{-2\kappa L}}. \tag{5.19}$$

The intensity transmission coefficient is the absolute square of the amplitude transmission coefficient $\zeta$. It reads, up to an exponentially small term in the denominator,

$$T=\frac{64k_0^2\kappa^4e^{-2\kappa L}}{4k_0^2\kappa^2(2\kappa-u)^2+[(2\kappa-u)(k_0^2-\kappa^2)-uV_0(e^{-2\kappa Z_0}+e^{-2\kappa(L-Z_0)})]^2}. \tag{5.20}$$

Since the potential is equal on both sides of the barrier, and the incoming and outgoing modes are the same, the flux transmission coefficient $\mathcal{T}$ equals the intensity transmission coefficient $T$. When $k_0^2=k_*^2\equiv V_0-u^2/4$, there is a resonance peak in the transmission. Since then $\kappa=u/2$, its height is

$$\mathcal{T}_{\max}=\mathcal{T}(k_*)=\frac{2k_*^2u^2}{V_0^2[1+\cosh u(L-2Z_0)]}. \tag{5.21}$$

From this equation, we can see that the tunneling transmission is maximal if the scatterer is positioned in the center of the barrier, $Z_0=L/2$. Then, the transmission coefficient is no longer exponentially small. Independent of the length of the barrier, its maximal value is

$$\mathcal{T}_{\max}[L/2]=\frac{k_0^2u^2}{V_0^2}=\frac{(V_0-u^2/4)u^2}{V_0^2}=1-\left(\frac{V_0-u^2/2}{V_0}\right)^2. \tag{5.22}$$

This phenomenon is called resonant tunneling. We see that $T$ is unity if $u^2=2V_0$. This occurs when the resonance energy is exactly half the barrier energy, $k_*^2=V_0/2$. We will now show how this feature of a truly 1D system persists in the quasi-one-dimensional waveguide.

### D. Resonant tunneling in a waveguide

The situation for impurity tunneling through a barrier in a waveguide is analogous to the 1D case if we can assume that the lowest subband is nondegenerate, i.e., there is a lowest subband $p_0$ and all other subbands are located at a higher energy. In that case, we can ignore tunneling through the higher subbands. We *do* need to include all subbands in the calculation of the return Green's function, as well as the reflection terms for the lowest subband. From (5.15), the return Green's function becomes

$$G(\boldsymbol{\rho}_0,Z_0,\boldsymbol{\rho}_0,Z_0)=\sum_{\mathbf{p}}\Psi_{\mathbf{p}}^2(\boldsymbol{\rho})G_{\mathbf{p}}(0)+G_{\mathbf{p}_0}(-Z_0)r_{\mathbf{p}}G_{\mathbf{p}_0}(Z_0)+G_{\mathbf{p}_0}(L-Z_0)r_{\mathbf{p}}G_{\mathbf{p}_0}(-L+Z_0). \tag{5.23}$$

We will use the abbreviations $\kappa_{\mathbf{p}}$ for the imaginary wave number inside the structure, $q_{\mathbf{p}}$ for the wave number outside

the structure, $r_{\mathbf{p}}$ for the internal (amplitude) reflection coefficient at the edge of the barrier

$$\kappa_{\mathbf{p}} \equiv \sqrt{\mathbf{p}^2 + V_0 - k_0^2}, \quad \kappa \equiv \kappa_{\mathbf{p}_0}, \tag{5.24}$$

$$q_{\mathbf{p}} \equiv \sqrt{k_0^2 - \mathbf{p}^2}, \quad q \equiv q_{\mathbf{p}_0}, \tag{5.25}$$

$$r_{\mathbf{p}} \equiv -2\kappa_{\mathbf{p}} \frac{q_{\mathbf{p}} - i\kappa_{\mathbf{p}}}{q_{\mathbf{p}} + i\kappa_{\mathbf{p}}}. \tag{5.26}$$

Thus, we can calculate the return Green's function, including the reflection terms

$$G(\boldsymbol{\rho}_0, Z_0, \boldsymbol{\rho}_0, Z_0) = \sum_{\mathbf{p}} \Psi_{\mathbf{p}}^2(\boldsymbol{\rho}) \left( \frac{1}{2\kappa_{\mathbf{p}}} - \frac{1}{2\sqrt{\Lambda^2 + \mathbf{p}^2}} \right) \tag{5.27}$$

$$- \Psi_{\mathbf{p}_0}^2(\boldsymbol{\rho}) \frac{e^{-2\kappa_{\mathbf{p}_0} Z_0} + e^{-2\kappa_{\mathbf{p}_0}(L - Z_0)}}{2\kappa_{\mathbf{p}_0}} \times \frac{q_{\mathbf{p}} - i\kappa_{\mathbf{p}}}{q_{\mathbf{p}} + i\kappa_{\mathbf{p}}}. \tag{5.28}$$

Neglecting the direct tunnelling term, we can calculate the transmission coefficient for a barrier with a scatterer at position $(\boldsymbol{\rho}_0, Z_0)$

$$T = \frac{16 q^2 \kappa^2 \tilde{u}^2 e^{-2\kappa L}}{(2 - u\tilde{R})^2 \kappa^2 V_0^2 - \kappa \tilde{u}(2 - u\tilde{R}) V_0 (q^2 - \kappa^2)[e^{-2\kappa Z_0} + e^{-2\kappa(L - Z_0)}] + \tilde{u}^2 V_0^2 [e^{-2\kappa Z_0} + e^{-2\kappa(L - Z_0)}]^2}, \tag{5.29}$$

with the abbreviations

$$\tilde{R} \equiv \sum_{\mathbf{p}} \Psi_{\mathbf{p}}^2(\boldsymbol{\rho}_0) \left( \frac{1}{2\sqrt{\mathbf{p}^2 + V_0 - k_0^2}} - \frac{1}{2\sqrt{\Lambda^2 + \mathbf{p}^2}} \right), \tag{5.30}$$

$$\tilde{u} \equiv u \Psi_{\mathbf{p}_0}^2. \tag{5.31}$$

The resonance condition now is $u\tilde{R} = 2$, where the peak flux transmission coefficient becomes

$$\mathcal{T}_{\max} = \frac{8 q_*^2 \kappa_*^2}{V_0^2 [1 + \cosh 2\kappa_*(L - 2Z_0)]}. \tag{5.32}$$

Again the maximum peak height occurs when the scatterer is located at the middle of the barrier

$$\mathcal{T}_{\max}[L/2] = 4 q_*^2 \kappa_*^2 / V_0^2 = 1 - \left( \frac{V_0 - 2k_*^2 + 2\mathbf{p}^2}{V_0} \right)^2.$$

It depends on the transversal scatterer position and on the scatterer strength only through the shift of the resonance position. Its maximal value is again unity.

We calculate the width of the resonance peak of (5.29). To do this we will need some derivatives:

$$\frac{\partial}{\partial k_0} \kappa_{\mathbf{p}} = -\frac{k_0}{\kappa_{\mathbf{p}}}, \tag{5.33}$$

$$\frac{\partial}{\partial k_0} q_{\mathbf{p}} = \frac{k_0}{q_{\mathbf{p}}}, \tag{5.34}$$

$$\frac{\partial}{\partial k_0} \tilde{R} = k_0 \sum_{\mathbf{p}} \Psi_{\mathbf{p}}^2(\boldsymbol{\rho}_0) \frac{1}{2\kappa_{\mathbf{p}}^3} \approx \Psi_{\mathbf{p}_0}^2(\boldsymbol{\rho}_0) \frac{k_0}{2\kappa_{\mathbf{p}_0}^3}. \tag{5.35}$$

The approximation for the derivative of $\tilde{R}$ is good if $\kappa_{\mathbf{p}_0}$ is much smaller than the other decay constants, which it is in a usual tunneling situation.

The denominator of (5.29) consists of three terms, the first two are zero at resonance. Half height occurs approximately when the sum of those terms equals the third term. The first term of the denominator is of second order in $\Delta k = k_0 - k_*$, the second term is of first order, but has a much smaller coefficient, so we will have to include both terms to determine the peak width. We solve

$$\frac{(\Delta k)^2}{2} \tilde{u}^2 \frac{k_0^2}{2\kappa^4} V_0^2 - (\Delta k) \tilde{u}^2 \frac{k_0}{\kappa^2} (q^2 - \kappa^2)(e^{-2\kappa Z_0} + e^{-2\kappa(L - Z_0)}) = \tilde{u}^2 V_0^2 (e^{-2\kappa Z_0} + e^{-2\kappa(L - Z_0)})^2 \tag{5.36}$$

to find the result

$$(\Delta k)_{\mathrm{FWHM}} = 4\kappa^2 \frac{e^{-2\kappa Z_0} + e^{-2\kappa(L - Z_0)}}{k_0 V_0} \sqrt{q^4 + \kappa^4} \tag{5.37}$$

$$\approx 4\kappa^2 \frac{e^{-2\kappa Z_0} + e^{-2\kappa(L - Z_0)}}{k_0}. \tag{5.38}$$

So the peak full width at half maximum, $(\Delta k)_{\mathrm{FWHM}}$, is exponentially small even if the scatterer is positioned near the center. Only through the resonance energy, determined by $u\tilde{R} = 2$, it depends on the $(x,y)$ coordinates of the scatterer or its scattering strength $u$. This means that of the three quantities that are easily accessible by experiment, the resonance position, height, and width, only the resonance position contains information about the scattering strength and $(x,y)$ position.

### E. Multiple scattering

Suppose that in the region $0 < z < d_z$ there is an *a priori* nonuniform density $n(x,y)$ of randomly placed, possibly resonant impurities. To first approximation, this causes the average subband Green's functions to obtain a self-energy term,

$$\Sigma_{\mathbf{p}} = \int d^2\boldsymbol{\rho} |\Psi_{\mathbf{p}}(\boldsymbol{\rho})|^2 n(\boldsymbol{\rho}) t(\boldsymbol{\rho}). \tag{5.39}$$

The self-consistent $t$ matrix can now be calculated by inserting the self-energy $\Sigma$ in (5.17). In order to describe diffusion, we need to define the ladder vertex $U$, which must obey a local conservation law (Ward identity) of the form of (2.30),

$$\mathrm{Im}\Sigma_{\mathbf{p}}=\sum_{\mathbf{p}'} U_{\mathbf{pp}'}\mathrm{Im}G_{\mathbf{p}'}=\sum_{\mathbf{p}'} U_{\mathbf{pp}'}\nu_{\mathbf{p}}. \tag{5.40}$$

This identity ensures flux conservation. We define the ladder vertex $U$ as

$$U_{\mathbf{pp}'}\equiv\int d^2\boldsymbol{\rho}\Psi_{\mathbf{p}}^2(\boldsymbol{\rho})\Psi_{\mathbf{p}'}^2(\boldsymbol{\rho})n(\boldsymbol{\rho})t(\boldsymbol{\rho})t^*(\boldsymbol{\rho}). \tag{5.41}$$

Then the Ward identity (5.40) indeed is satisfied, since

$$\begin{aligned} t(\mathbf{r})-\overline{t(\mathbf{r})}&=\frac{1}{u^{-1}-G}-\frac{1}{u^{-1}-G^*}\\ &=\frac{(u^{-1}-G^*)-(u^{-1}-G)}{(u^{-1}-G)(u^{-1}-G^*)}=tt^*(G-G^*), \end{aligned} \tag{5.42}$$

where we have written $G$ for $G(\mathbf{r},\mathbf{r})$. With the vertex function defined in (5.41), we can reproduce all results from Sec. II, if we make the following modifications:

(i) Wherever the expression $k_0^2-\mathbf{p}^2+i\Gamma_{\mathbf{p}}$ is used, we need to replace it by $k_0^2-\mathbf{p}^2+\Sigma_{\mathbf{p}}$, thereby incorporating the real part of the self-energy.

(ii) When the imaginary part $\Gamma_{\mathbf{p}}$ is used outside the propagator denominator, we should replace it by $\mathrm{Im}\,\Sigma_{\mathbf{p}}$.

(iii) The matrix $N_{\mathbf{pp}'}$, the second order Born approximation to the irreducible vertex, should be replaced by the full $t$-matrix approximation $U_{\mathbf{pp}'}$ defined in (5.41).

To find the correct self-energy, we need to solve $t(\boldsymbol{\rho})$ and $G_{\mathbf{p}}$ simultaneously, in general, we will need to do this numerically. As the equations are well-behaved in a physical situation, an iterative improvement method can be used. In Sec. VI, we will discuss an approach for a lattice model where a direct simulation of the scattering problem was performed.

The drops in the conductivity that can again be seen in the case of attractive scatterer, shortly before the opening of a new subband can be explained qualitatively as single scatterer resonances. The real part of the Green's function of the not-yet opened subband starts to diverge, which means it has to cross a resonant value, rendering the $t$ matrices of the individual scatterers imaginary and very large. Thus, the scatterers scatter more efficiently at these energies, thereby decreasing the conductance. As the resonance is position-dependent, there will not be a sharp drop in conductivity, but instead a smooth decrease. When the new subband opens, the density of states effects will cause a sharp drop in conductivity, which is already present in the second order Born approximation. For repulsive scatterers, no resonance exists and the conductivity will rise with increasing energy until the opening of the next subband, at which time it will drop again.

### F. Subband bottom transparency

For the case of a single scatterer in a channel, an interesting effect was observed by Chu and Sorbello[7] and by Bagwell:[16] when the energy is close to the bottom of a subband, the return Green's function is very large so that the $t$ matrix is small. As a result, there is almost no scattering. For the multiple scattering situation, the question that arises immediately is will the system become optically thin, so that *ballistic* transport determines the transmission coefficients?

Let the energy approach a subband bottom $k_0^2\approx\mathbf{p}_*^2$. The return Green's function $G_{\mathbf{p}_*}$ of this mode will become large, due to its quasi-one-dimensional square root divergency. The corresponding term in the denominator of (5.17) will dominate the other terms, except at the nodes of the corresponding subband wave function. If this wave function has no nodes, or the scatterer density is zero near those nodes, as can be the case for a waveguide with disorder only near the edges, the self-energy of the corresponding mode can be solved approximately:

$$\begin{aligned} \Sigma_{\mathbf{p}_*}&=\int d^2\boldsymbol{\rho}|\Psi_{\mathbf{p}_*}(\boldsymbol{\rho})|^2n(\boldsymbol{\rho})\frac{1}{u^{-1}-\Sigma_{\mathbf{p}'}|\Psi_{\mathbf{p}'}(\boldsymbol{\rho})|^2G_{\mathbf{p}'}(0)}\\ &\approx\int d^2\boldsymbol{\rho}|\Psi_{\mathbf{p}_*}(\boldsymbol{\rho})|^2n(\boldsymbol{\rho})\frac{-1}{|\Psi_{\mathbf{p}_*}(\boldsymbol{\rho})|^2G_{\mathbf{p}_*}(0)}\\ &=\int d^2\boldsymbol{\rho}n(\boldsymbol{\rho})2i\sqrt{k_0^2-\mathbf{p}_*^2+\Sigma_{\mathbf{p}_*}}=2in_{1\mathrm{D}}\sqrt{k_0^2-\mathbf{p}_*^2+\Sigma_{\mathbf{p}_*}}, \end{aligned} \tag{5.43}$$

where $n_{1\mathrm{D}}$ is the 1D scatterer density

$$n_{1\mathrm{D}}=\int d^2\boldsymbol{\rho}n(\boldsymbol{\rho}). \tag{5.44}$$

We see that (5.43) does not contain the scatterer strength $u$. It is valid for large values of $u$, as for very small scattering strength, the term $u^{-1}$ will not be neglegible compared to the return Green's function. Squaring (5.43) and requiring that the imaginary part of the self-energy stays positive, we find

$$\Sigma_{\mathbf{p}_*}=-2\,n_{1\mathrm{D}}^2+2in_{1\mathrm{D}}\sqrt{k_0^2-\mathbf{p}_*^2-n_{1\mathrm{D}}^2}\,. \tag{5.45}$$

This expression is of second order in $n(\boldsymbol{\rho})$. Although our theory is a first order approximation in $nt$, we can still use it because the $t$ matrix is so small near the subband bottom. This is the multiple scattering analog of the subband bottom transparency effect noted by Chu and Sorbello[7] and by Bagwell[16] for the case of a single scatterer: when the energy is at the subband bottom there is very little scattering, and the system may even become optically thin, in which case *ballistic* transport determines the transmission coefficients. We can calculate the behavior of the mean free path, which is, unlike the self-energy, usually easily experimentally accessible

$$\{l_{\mathbf{p}_*}\}^{-1}=2\mathrm{Im}\,(k_0^2-\mathbf{p}_*^2-2\,n_{1\mathrm{D}}^2+2in_{1\mathrm{D}}\sqrt{k_0^2-\mathbf{p}_*^2-n_{1\mathrm{D}}^2})^{1/2} \tag{5.46}$$

$$=2\mathrm{Im}\,(in_{1\mathrm{D}}+\sqrt{k_0^2-\mathbf{p}_*^2-n_{1\mathrm{D}}^2}). \tag{5.47}$$

This gives immediately

$$l_{*,\max}=\frac{1}{2\,n_{1\mathrm{D}}}. \tag{5.48}$$

If there are lower lying, already propagating modes, their mean free path can be much longer than this. Let us first consider the case where the scatterer density $n(x,y)$ is zero near the nodes of the mode wave function $\Psi_{\mathbf{p}_*}$. Then we can find the self-energy of the other modes by

$$\Sigma_{\mathbf{p}}=\Sigma_{\mathbf{p}_*}\int d^2\boldsymbol{\rho}\frac{n(\boldsymbol{\rho})}{n_{1\mathrm{D}}}\frac{|\Psi_{\mathbf{p}}|^2}{|\Psi_{\mathbf{p}_*}|^2}. \tag{5.49}$$

If we estimate the value of the integral to be roughly unity, we find for the mean free paths of the other modes

$$l_{\mathbf{p}}^{-1}\approx 2\,\mathrm{Im}\,(k_0^2-\mathbf{p}^2-2n_{1\mathrm{D}}^2+2in_{1\mathrm{D}}\sqrt{k_0^2-\mathbf{p}_*^2-n_{1\mathrm{D}}^2})^{1/2}\ . \tag{5.50}$$

Since $k_0^2-\mathbf{p}^2$ is much larger than the other terms, we can neglect terms of the order $(k_0^2-\mathbf{p}_*^2)/(k_0^2-\mathbf{p}^2)$ to find

$$\{l_{\mathbf{p}}\}^{-1}\approx 2\,n_{1\mathrm{D}}\frac{\sqrt{k_0^2-\mathbf{p}_*^2-n_{1\mathrm{D}}^2}}{\sqrt{k_0^2-\mathbf{p}^2}}, \tag{5.51}$$

where $\mathbf{p}_*^2\approx k_0^2$ is the newly opened mode and $\mathbf{p}^2\ll k_0^2$ for the already open modes. It is seen that this expression vanishes at the exact subband bottom, so the mean free path diverges and the transmission becomes ballistic in every mode except the newly opened one.

In practice, the scatterer density will not, in general, be exactly zero near the nodes of the wave functions. The $t$ matrix may be appreciable near the zeros of the wave function $\Psi_{\mathbf{p}_*}$ of the new mode, so that the approximation (5.50) cannot be made. This will have non-neglegible effects on the behavior of the other modes that do not have the same zeros. The corrections to the self-energy of the propagating modes that arise will be of the order $1/\sqrt{G_{\mathbf{p}_*}}$, which is very small near the subband bottom, so the resulting mean free path may, with these corrections, still become much larger than in the middle of the band. If it approaches the order of the system length, we can no longer use the results derived for optically thick systems. Thus, a sample may cross over from the semiballistic regime of multiple scattering to the ballistic regime of low-order scattering when the energy is near a subband bottom.

## VI. NUMERICAL SIMULATION

In order to look numerically at the effect of scatterers in a waveguide, we use a model which contains the essential physics of the continuum Schrödinger equation, while being ameanable to this kind of analysis. One such model is the Anderson Hamiltonian on a square lattice

$$\begin{aligned}H=\sum_{n_x,n_y}\{&-|n_x,n_y\rangle\epsilon_{n_x,n_y}\langle n_x,n_y|+|n_x+1,n_y\rangle\langle n_x,n_y|\\&+|n_x-1,n_y\rangle\langle n_x,n_y|+|n_x,n_y+1\rangle\langle n_x,n_y|\\&+|n_x,n_y-1\rangle\langle n_x,n_y|\}.\end{aligned}$$

By setting the hopping elements to unity, we define the unit of energy. The model has an upper and lower limit of energy $E=[-4,4]$ for the ordered case $\epsilon_{n_x,n_y}=0$. The electron like band structure that we are interested in starts at the band edge closest to $E=4$. The sign of the disorder parameter $\epsilon_{n_x,n_y}$ has been chosen, such that for positive values the scatterers are attractive and negative values repulsive. The conductance of this system can be calculated by simply transforming the Hamiltonian above into a set of transfer matrices, one for each layer, and multiplying them together to find the transfer matrix for the whole system. However, in the strong scattering regime where the conductance is very small, this method is unstable since half the eigenvalues grow exponentially and half decay. We, therefore, prefer to calculate the conductance from the Greens function, which either decays or grows. The method we use to calculate the Greens function was introduced by Lee and Fisher[18] and given for the general case by MacKinnon.[19] It consists of using Dysons equation to calculate the required elements iterativley by adding sucessive disordered layers. The general form for the relation between the Greens function elements and the transmission coefficients has been given by Baranger and Stone[20] and we use the Landauer-Buttiker formalism to calculate the conductance from these coefficients.

One of the major differences between the continuum model and the Anderson model is in the number of evanescent modes in a complete basis at the Fermi energy. The continuum model has an infinite number, whereas the Anderson model only has as many modes as there are lattice sites across the wire. We can easily accomodate our continuum theory to this band structure by taking an appropriate momentum cutoff function. In the simulations that we present in this paper, we have been interested in disordered systems which are long in comparison to the mean free path, but much narrower. In this limit, only the evanescent modes that have any appreciable probability amplitude between scattering events need be included. This makes the Anderson model an ideal candidate for this calculation. Comparison between these numerical simulations and our continuum model can be made without any free parameters, since the scatterer size is fixed by the requirement that each scatterer should occupy the volume of one lattice cell.

In Fig. 4, we compare the semiballistic theory (full line) with one realization of the Anderson model (dotted line). The sample configuration is that of a long, weakly disordered wire. In Fig. 5, the same is shown for repulsive scatterers. Both graphs also show the same curve calculated in the second order Born approximation, in which there is no difference between attractive and repulsive scatterers. The conductance is shown as a function of carrier energy, where the units of energy are related to the band structure of the lattice ($-4=$ zero energy, 0 band center). It is seen that the subband maxima have a round shape for attractive scatterers, while they are quite sharp for repulsive scatterers. Also, the conductance is lower for attractive scatterers. This can be explained as an effect of the scattering resonances that exist for attractive scatterers and are described in Sec. V.

The shape of the conductance graph is seen to be dependent on the sign of the scattering strength, its magnitude, and

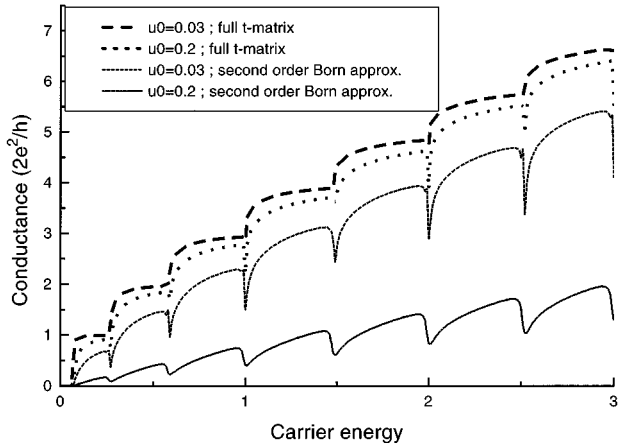


FIG. 6. Conductance of a $1000\times 11$ quantum wire with 5% attractive scatterers, calculated using the full $t$ matrix (dashed curves) or the second order Born approximation (dotted curves). For a bare scattering strength of 0.03, the second order Born approximation is a rather good approximation to the full $t$ matrix, for $u0=0.2$ there is a large difference.

the scatterer density. Depending on these parameters, the conductance trace can be either smooth, sawtoothlike (Fig. 5), or have steps (Fig. 6). These steps can be (much) smaller than the universal height $2e^2/h$ of steps in the conductance of ballistic devices, although they occur at the same energies.

It is also seen in these graphs that the second order Born approximation gives a conductance that is much lower than the full $t$ matrix, although it takes into account less scattering diagrams. This effect is shown for two different scattering strengths in Fig. 6. The explanation is that contributions of higher order scattering processes in the full $t$ matrix have the opposite sign of the lowest order contribution.

In Figs. 7 and 8, conductance of shorter samples with a relatively high density of scatterers are shown. The good agreement between our theory and the numerical date (average over ten samples) demonstrates that our model, which

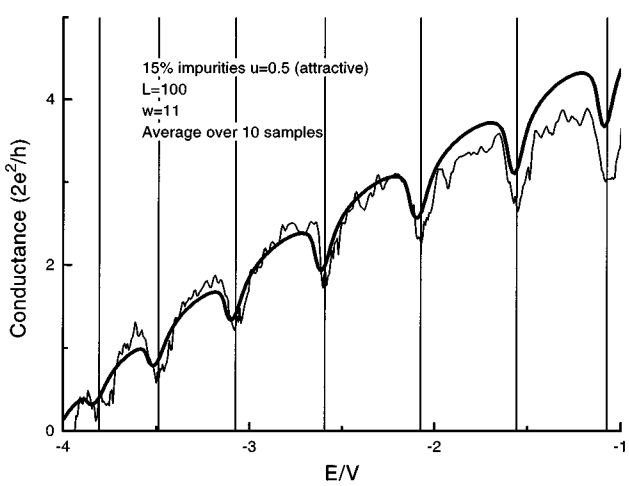


FIG. 7. Conductance of short quantum wires with a large amount of attractive scatterers. The thick line represents the semiballistic theory, the thin line is an average over ten numerical simulations.

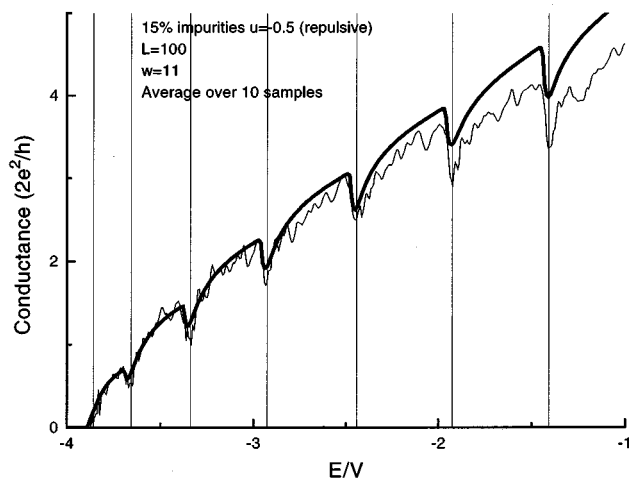


FIG. 8. Conductance of short quantum wires with a large amount of repulsive scatterers. The thick line represents the semiballistic theory, the thin line is an average over ten numerical simulations.

assumes pointlike scatterers, is still good at finite volume fractions.

In Fig. 9, we see the contact resistance term $R_c$ and the extrapolation length $z_0$, which gives rise to this contact resistance. It is clearly seen that $z_0$ is highly nonuniform and varies within each subband with a small dip attributed to scattering resonances (the return propagator being small and real there), a peak owing to a weak form of subband bottom transparency (the propagator being large and real, so that scatterers cannot be resonant and scattering is slightly suppressed) and a steep drop caused by the sudden increase in density of states as the propagator crosses over from large and real to large and imaginary. Note that the contact resistance $R_c$ has a much smoother behavior. It occurs since the conductivity $\sigma$ essentially varies in the same way as $z_0$.

The extrapolation length $z_0$ is a weighted average of the mode mean free paths (2.45), so it is of the order of one mean free path. Since our theory presently does not include quantum localization effects, it does not remain valid for samples which are many mean free paths in length. Therefore, in the regime where the semiballistic theory is valid, the influence of the contact resistance term in Eq. (3.4) will always be important. Figure 10 shows an example of a wire, which is so long that localization effects can no longer be neglected.

Nikolić and MacKinnon[21] discuss the conduction of quantum wires with a large amount of boundary roughness and a number of scattering islands in the bulk. They describe the wires with a tight binding lattice model, in which some lattice sites are nonconducting (infinite potential). The conduction is then calculated numerically and averaged over a large number of configurations. Our model can be compared to their data for the case when there is no boundary roughness. In their Fig. 7 our theory would predict a slightly higher average conductance (about 1 times $e^2/h$ higher), while the qualitative shape of the curve is about the same. It should be noted that a sample with these dimensions contains on the

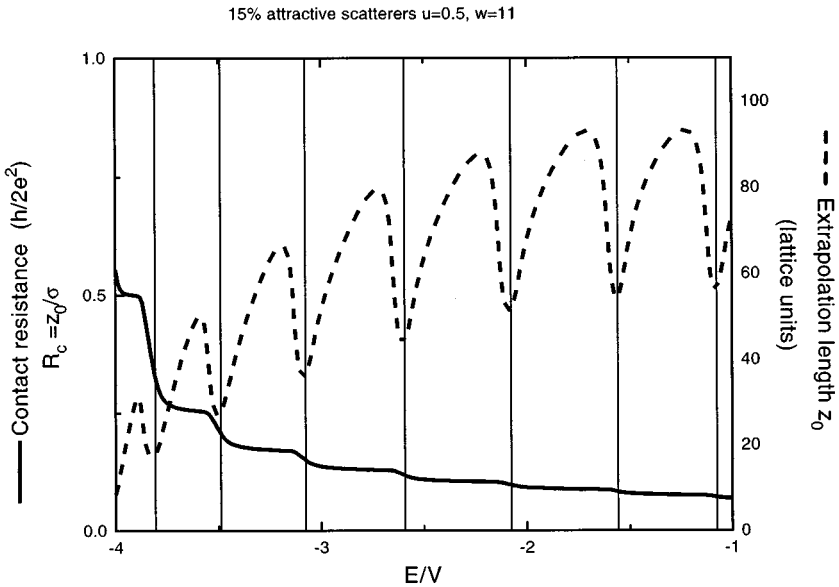


FIG. 9. Extrapolation length $z0$ and contact resistance $R_c = z_0/\sigma$ of a modestly disordered wire.

average only 5 scatterers, and our extrapolation length $z_0$ is about 1.5 times the sample length $d_z$. Therefore, this sample is only in the crossover region between the ballistic regime and the regime of semiballistic transport.

The data of Nikolić and MacKinnon[21] also shows that the localization length for samples containing these strong scatterers is only a few times larger than the mean free path, which means that the range of validity of our analytic model, which presently does not contain localization corrections, is rather limited. Many experimentally accesible systems fall within this range though. Also, for weaker scatterers (with finite potentials), the localization length will be longer, extending the range of validity of our model to longer samples.

Although our model assumes the scatterers are in the bulk of the wire, it can also be used to study qualitatively the effects of surface roughness, described as a high concentration of scatterers near the surfaces, with a vanishing scatterer density in the bulk. In this case, there will be a strong subband bottom transparency effect when the second subband opens, as the scatterer density vanishes near the node of the second subband wave function. This gives rise to a peak in the transmission of the wire at the exact bottom of the second subband, as can be clearly seen in Figs. 3 and 10 of Ref. 21. This peak is now well explained by our theory.

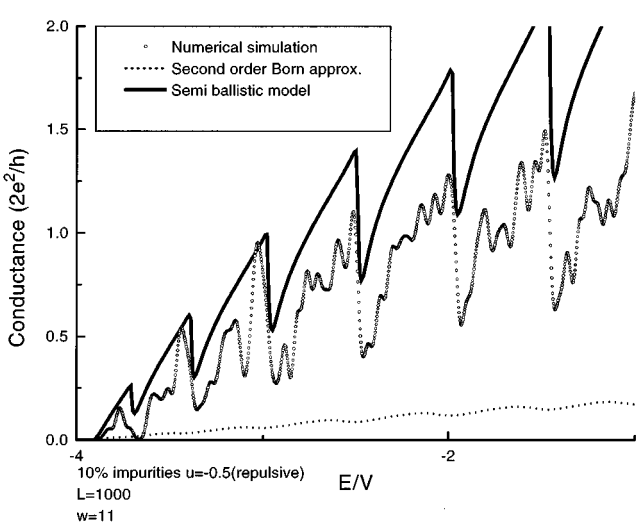


FIG. 10. Conductance of a long quantum wire with a high density of strong scatterers. At this point, our simple model breaks down as localization corrections become important. The effective mean free path is in the order of one tenth of the wire length.

## VII. DISCUSSION

We have found expressions for average transmission properties of two geometries of semi-ballistic devices, the waveguidelike geometry and the double-barrier structure. Both geometries apply to optical systems and quantum-electronical systems. Partly such systems are already experimentally accessible, while other realizations are expected to become available soon.

Steps in the conductance of electronic systems are predicted, together with remarkable drops shortly before a new subband opens. These drops have been described before in Ref. 13. We notice that for systems containing pointlike scatterers, the behavior of the conductance near these drops depends on the sign of the scattering length.

Our expressions go beyond the second order Born approximation to the $t$ matrix of the individual scatterers (or random Gaussian potentials) and can, therefore, include scattering resonances. Divergencies are dealt with in a physically meaningful way. It is shown that in a narrow waveguide, the second order Born approximation is not always good, even when it is accurate for the same scatterers in wide three-dimensional systems. Comparing our theory to numerical solutions of an Anderson model, we find good agreement in the regime where localization effects can be neglected.

*Note added in proof.* Very recently, García-Mochales *et al.*[22] have also presented numerical calculations in the semiballistic regime. Their results for the conductance are in agreement with ours, while these authors also focus on enhanced forward and backscattering.

**ACKNOWLEDGMENTS**

The interest in this work arose from discussions with the late Shechao Feng, which are gratefully acknowledged. Th.M. N. also benefited from discussion with N. Garcia, J.J. Saens, P. García-Mochalez, B.A. Altshuler, and I.V. Lerner, and for hospitality at the University of Madrid, where part of this work was performed. His work was made possible by the Royal Dutch Academy of Arts and Sciences (KNAW). This work was also supported by the NATO, Grant No. CRG 921399.

[1] C.W.J. Beenakker and H. van Houten, in *Solid State Physics: Advances in Research and Applications*, H. Ehrenreich and D. Turnbull (Academic, San Diego, 1991), Vol. 44.

[2] B.J. van Wees, H. van Houten, C.W.J. Beenakker, J.G. Williamson, L.P. Kouwenhoven, D. van der Marel, and C.T. Foxon, Phys. Rev. Lett. **60**, 848 (1988).

[3] E.A. Montie, E.C. Cosman, G.W. 't Hooft, M.B. van der Mark, and C.W.J. Beenakker, in *Analogies in Optics and Micro-Electronics*, edited by W. van Haeringen and D. Lenstra (North-Holland, Amsterdam, 1991), p. 149.

[4] Th.M. Nieuwenhuizen, Europhys. Lett. **24**, 269 (1993).

[5] J. Masek, P. Lipavsky, and B. Kramer, J. Phys. Condens. Matter **1**, 6395 (1989).

[6] J. Faist, P. Guéret, and H. Rothuizen, Phys. Rev. B **42**, 3217 (1990).

[7] C.S. Chu and R.S. Sorbello, Phys. Rev. B **40**, 5941 (1989).

[8] P. Guéret, C. Rossel, E. Marclay, and H. Meier, J. Appl. Phys. **66**, 278 (1989).

[9] Th.M. Nieuwenhuizen, A. Lagendijk, and B.A. van Tiggelen, Phys. Lett. A **169**, 191 (1992).

[10] G.D. Mahan, *Many-Particle Physics* (Plenum, New York, 1981).

[11] D. Vollhardt and P. Wölfle, Phys. Rev. B **22**, 4666 (1980).

[12] Th.M. Nieuwenhuizen and J.M. Luck, Phys. Rev. E **48**, 569 (1993).

[13] M. Suhrke, S. Wilke, and R. Keiper, J. Phys. Condens. Matter **2**, 6743 (1990).

[14] R. Berkovits and S. Feng, Phys. Rev. B **45**, 97 (1992).

[15] J.F. van Diejen and A. Tip, J. Math. Phys **32**, 630 (1991).

[16] P.F. Bagwell, Phys. Rev. B **41**, 10 354 (1990).

[17] P.L. McEuen, B.W. Alphenaar, and R.G. Wheeler, Surf. Sci. **229**, 312 (1990).

[18] P.A. Lee and D.S. Fisher, Phys. Rev. Lett. **47**, 882 (1981).

[19] A. MacKinnon, Z. Phys. B **59**, 385 (1985).

[20] H.U. Baranger and A.D. Stone, Phys. Rev. B **40**, 8169 (1989).

[21] K. Nikolić and A. MacKinnon Phys. Rev. B **50**, 11 008 (1994).

[22] P. García-Mochales, P. A. Serena, N. Garcia, and J. L. Costa-Krämer, Phys. Rev. B **53**, 10 268 (1996).